International
Progress Report

IPR-99-09

Äspö Hard Rock Laboratory

Prototype Repository DFN Model No. 1

Jan Hermansson, Martin Stigsson
Golder Grundteknik, Sweden

Alec Pringle
Golder Associates (UK) Ltd, United Kingdom

June 1999

Svensk Kärnbränslehantering AB
Swedish Nuclear Fuel
and Waste Management Co
Box 5864
SE-102 40 Stockholm Sweden
Tel 08-459 84 00
+46 8 459 84 00
Fax 08-661 57 19
+46 8 661 57 19

Äspö Hard Rock Laboratory

Äspö Hard Rock Laboratory

Prototype repository DFN
Model No. 1

Jan Hermansson, Martin Stigsson
Golder Grundteknik, Sweden

Alec Pringle
Golder Associates (UK) Ltd, United Kingdom

June 1999

Keywords: DFN, fracture, prototype repository, inflow

RAPPORTNUMMER
IPR-99-09

TILLHÖR/REG.N
F63K

FÖRFATTARE
J Hermansson, A Pringle, M Stigsson

DATUM

TILLSTYRKT
Lars-Olof Dahlström
Ingvar Rhén

DATUM
1999-05-20
1999-05-20

GODKÄNT/FASTSTÄLLT
Olle Olsson

DATUM
1999-11-04

PROTOTYPE REPOSITORY DFN MODEL NO.1

Jan Hermansson[1]
Alec Pringle[2]
Martin Stigsson[1]
(1) Golder Grundteknik, Solna, Sweden
(2) Golder Associates (UK) Limited, Nottingham, United Kingdom

Abstract

A discrete feature network model, DFN, has been set up to simulate inflow to the pilot holes of the 2nd drill campaign and the planned deposition holes in the Prototype repository. Input data to the simulation has deliberately been kept at a generic level, not including any deterministic information from the repository volume. Structural and hydraulic information have largely been derived from the TRUE Block Scale volume south of the Prototype repository to simulate a future situation when there are no detailed information of the rock mass of interest. Information from the 1st drill campaign show that fracture data from the TRUE Block Scale volume are comparable to data from the Prototype repository volume.

Model simulations predict the conductive fracture frequency, P_{10c}, to around 0.34 fractures per meter in vertical boreholes. The fracture trace length per unit area, P_{21c}, on the walls of the deposition holes is estimated to 0.4 m/m^2.

Inflow to the vertical pilot holes in the repository are on average 0.07 l/min. Inflow to the 1.75 m wide and 8 m deep deposition holes equals on average 0.15 l/min.

The simulations show that if only steep fractures are considered to be conductive the model can be calibrated to measured inflow to the Prototype tunnel and the pilot holes of the 1st drill campaign without using any skin effects.

Table of contents

Figures and tables

1 Introduction

1.1 The Prototype repository

1.1.1 General objectives

The prototype repository is focused on testing and demonstrating as many of the functions of a real repository as possible. Equipment and technique of deposition and storage will be tested in natural conditions as well as numerical models aimed at predicting structural and hydraulic behaviour in the vicinity to the repository.

The major objectives for the Prototype Repository are:

- To test and demonstrate the integrated function of the repository components under realistic conditions in full scale and to compare results with models and assumptions
- To develop, test and demonstrate appropriate engineering standards and quality assurance methods
- To simulate appropriate parts of the repository design and construction process

The geological characterisation of the repository rock volume will be made in three stages where each stage is intended to contribute to more details aimed at localising the deposition holes. The characterisation stages involve mapping of the tunnel section, pilot and exploratory boreholes and finally drilling of the deposition holes.

1.1.2 Prototype DFN model objectives

A future repository will be characterised in phases where predictions are being made from data achieved at different stages. This report presents a modelling approach where we simulate the first of a series of predictions based on data with increasingly more detailed information from the rock mass. Not only can this approach be used for predictions of the geosphere characteristics but also to evaluate how the probability of making successful predictions increases by collecting more detailed data.

The objectives for the modelling approach are:

- to describe the statistical fracture distributions used in the modelling
- analyse and describe the fracture data assembled by the 1st drill campaign (10 pilot holes and 3 core drilled boreholes).
- compare fracture data assembled by the 1st drilling campaign with the existing TRUE Block Scale DFN data set as presented by Hermanson et al. (1997) and Follin et al. (1997).
- implement boundary conditions, DFN parameters, deposition holes, tunnels and applicable parts of the site scale structural model by Rhén et al. (1997) into the numerical model.
- predict fracture statistics of the 2nd drill campaign and in the deposition holes.
- predict inflow to the planned prototype deposition holes.

The modelling is performed using the Discrete Feature Network concept, DFN, with the codes FracMan and MAFIC, developed by Golder Associates.

2 Concept of the DFN modelling approach

Discrete fracture modelling is useful for modelling possible geological conditions when there are little or no data as well as when more detailed data are available. FracMan is developed to model the geometry of discrete features and provides an integrated environment for the entire process of statistically analyse data to modelling the network geometry in stochastic simulations. The program package FracMan consists of two main sub modules, FracSys and FracWorks. FracSys is used in the initial data analysis and derivation of input fracture parameters whereas FracWorks simulates the geometric networks in a stochastic manner and provides network geometry's for the finite element flow solver MAFIC describes further down. Table 2-1 summarises the FracMan input requirements and the FracSys modules used to derive the required information.

Table 2-1. FracMan data requirements.

FracMan input requirement	**Raw data**	**FracSys module**
Fracture set definition	Borehole logs Fracture trace maps (orientation, infilling, termination, mineralization, size, etc.)	ISIS
Fracture set orientation	Borehole logs Fracture trace maps (orientation)	ISIS
Fracture set termination probability	Fracture trace maps	HeterFrac
Fracture set location conceptual model	Fracture trace maps (trace co-ordinates)	HeterFrac
Fracture set size distribution	Fracture trace maps (trace length)	FracSize
Fracture set transmissivity distribution	Packer test interval Transmissivities	OxFilet
Fracture set conductive intensity	Packer test interval Transmissivities	OxFilet
Fracture network hydraulic connectivity	Packer test transient results	FracDim

FracWorks are used to generate a wide variety of discrete features in a stochastic manner. Deterministic features, tunnels, packer sections etc can be included in the model. Fracture statistics can be extracted from the three dimensional fracture networks and calibrated with observed fracture data in boreholes, outcrops or tunnels. FracWorks realisations can be saved for further use in other programs dealing with exploration simulation, pathway analysis and ground water flow and solute transport modelling.

MAFIC (**Ma**trix/**F**racture **I**nteraction **C**ode) is used to simulate transient flow and solute transport through three-dimensional rock masses with discrete fracture networks derived by FracMan. MAFIC handles all types of network geometry's and objects modelled by FracMan such as tunnels, deterministic objects, deposition holes etc.

A more detailed description of the concept of the software package FracMan and MAFIC is given in appendix A.

3 Available Prototype Repository data

This chapter presents the two available sets of input data to the Prototype DFN model:

1. fracture data that has been collected in the 1st drilling campaign of the Prototype repository

2. a borehole and tunnel data set from the TRUE Block Scale volume adjacent to the Prototype repository

The data is selected to simulate a future situation where local knowledge of a deposition tunnel is limited. In this particular project, data outside the Prototype repository volume is derived from the Äspö HRL site scale model and from the TRUE Block Scale project, which is carried out in the rock mass just south of the tunnel section where the Prototype repository is situated, c.f. Figure 3-1.

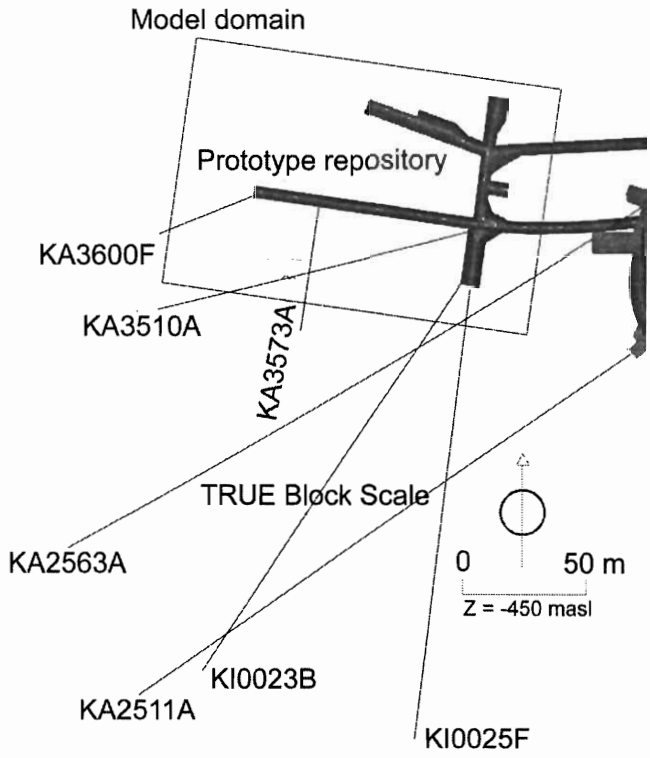

Figure 3-1. *Localisation of the Prototype Repository and the size of the modelling domain. Data from the TRUE Block Scale project has been used as input to the stochastic model.*

3.1 Fracture statistics of the 1st drilling campaign

The 1st drilling campaign comprises the drillings of ten sub-vertical pilot core holes in the floor of the TBM tunnel and three core boreholes with varying orientation. The data from this drill batch has been delivered by SKB through SICADA 980506 and contains information on the positions of fractures in each borehole. Figure 3-2 show the fracture frequency of the short, 8 m pilot core holes in the floor of the TBM tunnel as well as the frequency of the longer core boreholes which are more or less gently plunging. There is a tendency that steep fractures dominate fracturing in the rock block, as shall be seen when data from the TRUE Block Scale site are presented below. This is also evident when observing the difference in average frequency between the gently dipping cored boreholes compared to the short steep pilot holes, c.f. Figure 3-2. The average fracture frequency of the gently dipping boreholes is more than twice the average of the vertical boreholes.

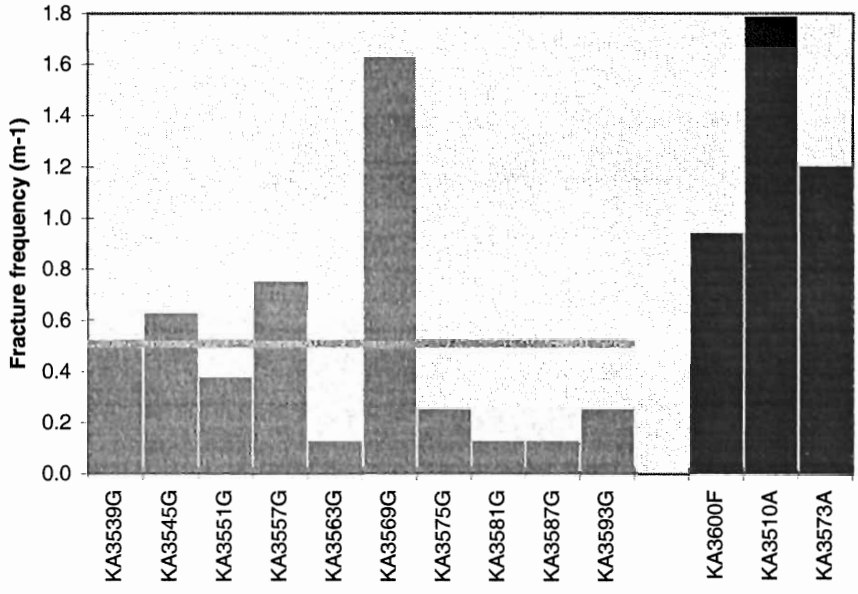

Figure 3-2. *Fracture frequency of the boreholes drilled in the 1st drilling campaign. The line indicates the average fracture frequency, 0.5 m^{-1}, in the subvertical 8 m long pilot core holes.*

Six positions at the locations close to certain pilot core holes are reserved for the placement of six deposition holes. Co-ordinates in Table 3-1 give tentative centre point for six deposition holes eight meters deep and 1.75 m wide.

Table 3-1. Co-ordinates of the centre points of the deposition holes.

Deposition hole	Eastings	Northings	Elevation
no. 1	1920.7	7269.6	-449.1
no. 2	1914.7	7270.4	-448.9
no. 3	1897.0	7273.0	-448.6
no. 4	1891.0	7274.0	-448.5
no. 5	1885.1	7274.8	-448.3
no. 6	1879.2	7275.7	-448.2

3.2 Inflow to tunnels and boreholes from the 1st drill campaign

Inflows in the HRL are measured at weirs collecting water in sections along the tunnel system. In this report, inflow data comes from tunnel sections in the vicinity of the Prototype repository; i.e. the F-tunnel and from the Prototype tunnel section at 3521-3600 m. The inflow data in the F-tunnel is based on the period July 1995 to October 1996. Inflow data for the Prototype repository is sampled from the period of 18 August 1997 to 1 September 1997. The difference in sampling period is due to the fact that data has to come from a hydraulically undisturbed period and that the excavation of the tunnels was made at different periods. Inflows are approximated to 10 l/min for the F-tunnel and 6.3 l/min for the Prototype repository tunnel respectively.

Rhén and Forsmark (1998) have performed a series of hydraulic packer tests in the ten drilled pilot core holes and estimates the flowrates (Q_{tot}) on average to 0.04 l/min, c.f. Figure 3-3. The inflows between different boreholes vary between 10^{-7} to 10^{1} l/min. The average is a relatively small inflow compared to what can be observed in other boreholes at Äspö. The large variation suggests that inflow will possibly increase dramatically if a highly conductive feature is intersected.

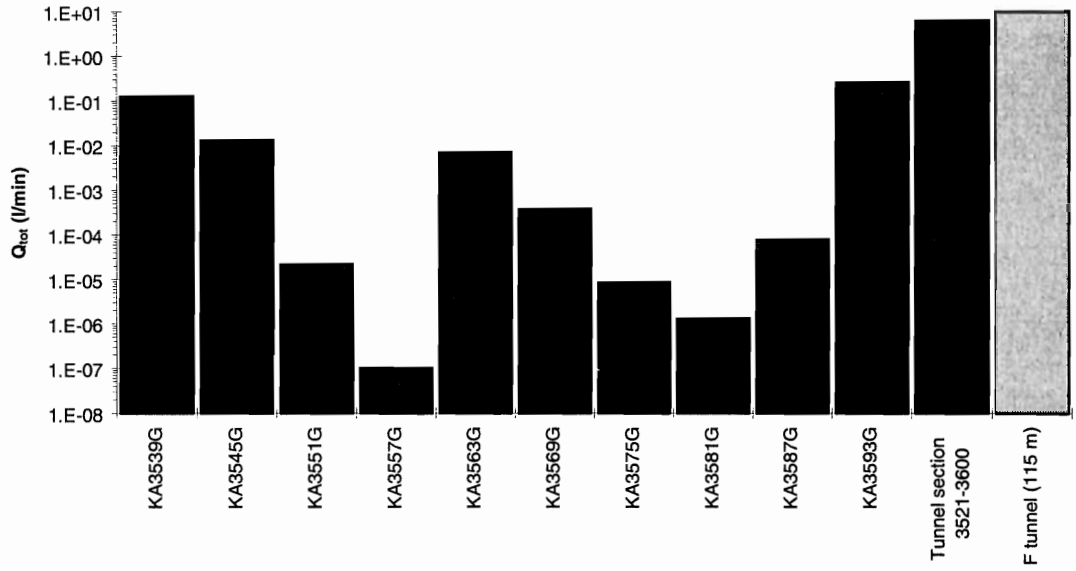

Figure 3-3. *Estimated flowrates from the ten pilot core holes in the 1st drilling campaign, after Rhén and Forsmark (1998), prototype tunnel and F-tunnel.*

3.3 Fracture statistics of the TRUE Block Scale volume

The TRUE Block Scale project focuses on a 500 m rock block lying south of the Prototype repository. The target for this project is to study transport and retention mechanisms within a fracture network at the scales of 50 m. This block has initially been penetrated and sampled by three long cored boreholes. A large number of hydraulic tests have been carried out as well as a major effort to map the conductive structures in the block.

Hermanson et al. (1997) and Follin and Wei (1997) describe and evaluate the fracture statistics of the TRUE Block Scale volume after the characterisation of boreholes KA2511A, KA2563A and KA3510A. They have, based on this information, derived a set of DFN parameters to be used in the flow modelling of the experimental site. Below follows an extensive summary of their main findings.

3.3.1 Fracture orientation

The separation of fractures into different sets based on geometric or geological parameters can significantly improve the understanding of the fracture network and thus also increase performance of a DFN model. Previous studies of the Äspö HRL tunnel data (La Pointe et al., 1993, 1995; Munier, 1995) have put great efforts in statistically separating fractures into sets based on fracture mineralogy, orientation, trace length, termination modes, surface roughness and kinematical evidence etc. However, the main conclusion is that the fracturing is not or only weakly correlated to most fracture properties, except for a slight increase in the trace length for water bearing fractures. However, the coupling of fracture orientation to hydraulic properties is not fully understood and still needs to be investigated. An example of the coupling of conductive fractures and the fracture network is given by Rhén et al (1997) which couples direction of a large amount of short pilot boreholes drilled at the front of the advancing access tunnel to inflow. The result of this investigation revealed that transmissivity is higher in fractures with a north westerly orientation than in other directions. This is also the direction of the major part of the steep fractures measured in the tunnel as well as the direction of the principal component of the horizontal stress.

The characterisation of the rock mass fracturing within and close to the TRUE Block Scale site was based on the observations made in the three boreholes, KA2563A, KA3510A and KA2511A and in the last 200 m of the TBM tunnel. The TBM data is considered to be of high quality as it covers a larger volume and is thus less affected by an orientation bias and also contains information on fracture trace length which is necessary for fracture size estimations. However, the TBM data set is a small sample, less than 300 fractures and should therefore be used with caution. For the purpose of an analysis of the orientation and clustering of the fractures in the site, drill core data from KA2563A and KA3510A are preferred as these boreholes were mapped with the BIPS

system which give a higher resolution of individual fracture orientations than boreholes mapped with the petrocore mapping system (KA2511A).

Hermanson et al. (1997) performed an orientation analysis with the purpose of finding statistical or geological evidence to separate the observed orientations of fractures into sets with possibly different properties. The guiding parameter for such a separation can be orientation alone, or a combination of orientation and other geological and physical properties. Figure 3-4 shows the stereo plot of the poles to the fracture planes observed in KA2511A, KA2563A, KA3510A. The orientation bias has been geometrically corrected using the Terzaghi correction (Terzaghi, 1965 and appendix A). This technique balances the orientation bias such that fractures at acute angles to the borehole axis are enhanced in number according to a weighting factor that is inversely proportional to the probability of intersecting those fractures with the borehole. To avoid that fracture normals with acute angles close to 90° completely dominates the corrected set, the weighting factor has to be constrained to a maximum number of around 10 according to studies by Yow (1987). For this study, a maximum correction factor of 5 has been used in all analyses, based on previous experience from La Pointe *et al.* (1995) and Dershowitz *et al.* (1996).

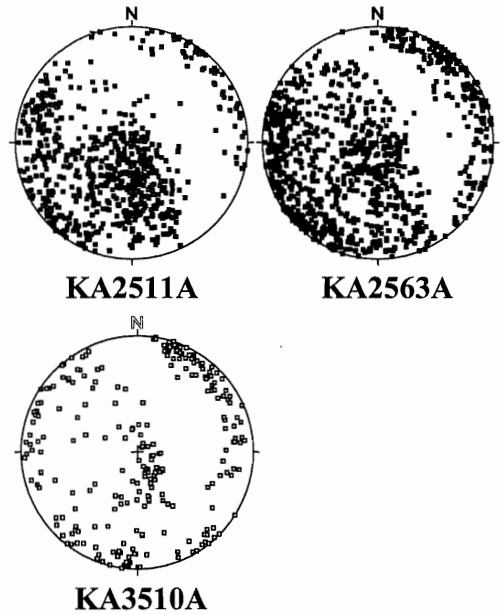

Figure 3-4. *Lower hemisphere projection of poles to fracture planes in the TRUE Block Scale volume (equal area or Schmidt plot). Two steep fracture sets with a north westerly orientation as well as one subhorizontal fracture set are observable in the plots.*

The main reason for separating observed fractures into sets would be to conclude whether parameters important for controlling flow in the network are set specific. Fracture size and fracture termination are two geometric parameters that would significantly influence the connectivity of the network and thus indirectly affect the conductivity through the network. As fracture trace length is missing in the borehole data information has to be found elsewhere in the vicinity of TRUE Block Scale site.

Figure 3-5 shows a stereo plot of the last section of the TBM tunnel where it is clear that the same three sets of fracturing dominate here as in the borehole data, c.f. Figure 3-4. Statistical fracture set separation of the fractures in the last section of the TBM tunnel using the ISIS pattern recognition approach in FracSys show a great similarity to orientations of the previously separated sets. The main difference being that sets in the TBM are somewhat more clustered than in the boreholes, c.f. Figure 3-5.

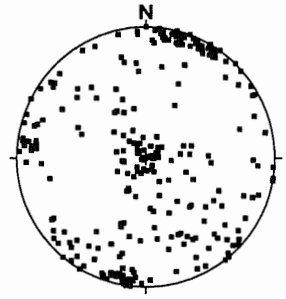

Figure 3-5. *Stereo plot of poles to fracture planes in the last 120 m of the TBM tunnel.*

The statistical set separation coincides with the fracture set separation done by visual inspection together with experience from fracture mapping elsewhere in the Äspö bedrock. It seems that fracture set 3, c.f. Table 3-2, in both the TBM and in the borehole data has the best correlation with a Fisher model of all sets. Set 1 in the borehole data is poorly defined in comparison to the tighter, more defined cluster in the TBM data. It is difficult to say whether this is a local variation or just an artefact by the bias correction method. At this stage it only seems obvious that there is two steep sets and one subhorizontal. The distributional data presented in Table 3-2 should be interpreted and used with care.

However, Hermanson et al. (1997) and Follin and Wei (1997) cannot successfully find any clear evidence for fracture set dependence on neither size nor transmissivity. This result implies that it is computationally more effective to generate DFN models based on one bootstrapped orientation distribution, i.e. to generate fractures in the network that exactly follows the total measured fracture orientation distribution rather than generating three sets of fractures with the same statistics as given in Table 3-2. However, even if previous investigations have failed at finding correlation's to fracture sets it is not impossible that such relations exist. We know that the regional stress filed is parallel to the main direction of fracturing (NW) and that the transmissivity is somewhat higher in this direction. This could be tested with fracture set separation. Further, the possible hydraulic character of subhorizontal fracturing is not fully understood today. Fracture sets with different transmissivity distributions may help understand directional transmissivity dependencies. It is therefore considered suitable to test and evaluate a few of these cases using network models with differently parameterised fracture sets. However, if no fracture set dependencies are found, it is more efficient to generate networks based on bootstrapped fractures.

Table 3-2. Statistical separation of fracture sets of the TRUE Block Scale data set according to Hermanson et al. (1997).

Fracture set 1		
Orientation (trend, plunge)	117.9	12.9
Fisher K	5.64	
Kolmogorov- Smirnov (K-S, %)	0.16	38.5
Trace length statistics		
Mean	8.359375 m	
Sample Variance	27.85475	
Kurtosis	-0.56353	
Skewness	0.894438	
Minimum	2.1 m	
Maximum	20.3 m	
Count	77	
Fracture set 2		
Orientation (trend, plunge)	200.4	2
Fisher K	15.75	
Kolmogorov- Smirnov (K-S, %)	0.163	4.6
Tracelength statistics		
Mean	7.916901 m	
Sample Variance	22.19228	
Kurtosis	-0.14086	
Skewness	0.904207	
Minimum	1.8 m	
Maximum	20.5 m	
Count	305	
Fracture set 3		
Orientation (trend, plunge)	186.5	81.1
Fisher K	13.6	
Kolmogorov- Smirnov (K-S, %)	0.095	79.7
Trace length statistics		
Mean	8.873913 m	
Standard Deviation	116.1037	
Kurtosis	17.26704	
Skewness	3.76579	
Minimum	1.4 m	
Maximum	65.5 m	
Count	275	

3.3.2 Fracture size

The general shape of a fracture in three dimensions is essentially unknown. We can observe traces and cuts on walls and outcrops but the complete shape of the fracture remains invisible. For conceptual purposes, fractures can be simplified as disks, and their sizes[1] can be estimated by looking at the trace length on outcrops and tunnel walls. Size is important to the connectivity in the fracture network and thus indirectly to the overall conductivity of the model domain.

To estimate fracture size from measured fracture traces it is possible to use the fact that for a particular fracture orientation, tunnel orientation and tunnel cross-section, the probability that a fracture trace could be mapped all the way around the tunnel surface is a function of fracture size. Size can thus be estimated by defining how large part of a tunnel surface a fracture intersects.

According to Hermanson et al. (1997), there exist two different sets of data from the last section of the TBM tunnel, 3480-3600 m. Traces on the tunnel walls have been mapped by site geologists through visual inspection just after blasting of a new section. The two data sets have its origin in the mapping technique of the geologists. The first data set consists of hand drawn maps of the traces in the tunnel. These maps have then been digitised at the site, and later converted by VBB Viak to 3D co-ordinates as reported in Follin and Hermanson (1996). These sketched traces are here referred to as the VBB Viak data set. The second data set comes from the estimation of the trace length performed by the same geologist simultaneously as he draws the trace map. This estimate is then recorded in SICADA, and is here referred to as the SICADA data set. Ideally they should be identical. However, estimating the length of an object by sketching is generally easier than estimating with numbers. The effect of this can be seen by looking at the mean trace lengths from these different data sets,

- SICADA data set, mean trace length 5.5 m.
- VBB Viak data set, mean trace length 8.3 m

The TBM tunnel is circular and has fracture traces all around its perimeter. Unfortunately, when the original mapping was performed in the tunnels of the HRL, fracture traces less than one meter were excluded (not recorded). This trace truncation implies that fractures with a radius less than 0.5 m intersecting the tunnel can not be analysed as traces are not measured. It also implies that traces of larger fractures, which are just intersecting a small part of the tunnel wall (< 1 m) are truncated.

[1] In FracMan, fracture size is expressed as the equivalent radius of a circular disk with the same area as the fracture, independent of shape.

Hermanson et al. (1997) used two different methods to estimate the size distribution. The first method, after La Point et al. (1993), is shortly summarised below:

1. Intersection statistics from the field observations were produced using 16 panels on the walls of the TBM tunnel (i.e. resembling a 16 sided tunnel)
2. A DFN model was generated with parameters according to Table 3-2.
3. A 16 sided tunnel resembling the size and orientation of the TBM tunnel was inserted into each network realisation of the DFN models.
4. For each trace the number of panels intersections were calculated.
5. A correlation analysis of the 16 panel intersection statistics between the simulations and the observations show in which mean size window there is best correlation of trace statistics.

The input data for this analysis is the VBB Viak data set. The analysis was subjected to the following rationale: Traces shorter than a meter was discarded from the analysis as the observations are subjected to such a truncation. However, a non-truncated size distribution was used in the stochastic network realisations, as truncation of traces does not necessarily imply that fractures of sizes less than 0.5 m in radius does not exist. The latter is certainly true, as can be observed in drill cores and on tunnel walls. But by using a non-truncated size distribution and only truncating the traces on the tunnel wall, we may enhance our possibility to recreate what has been observed also in the fractured drill cores. The analysis is based on calculating number of panels intersected by fractures and comparing the observed panel intersections with simulated panel intersections. There may be several weaknesses to such a method, such as correlation to a small observed sample with an uneven distribution, and lack of panel intersection statistics for fracture sets with an extremely acute angle to the tunnel axis. However, one may also argue that small samples are always subject to weak statistical significance.

Hermanson et al. (1997) tried mean sizes radius 1 - 12 m and standard deviation 1 - 5 m. Figure 3-6 to Figure 3-8 shows the correlation of the intersection statistics for the three sets defined in Table 3-2.

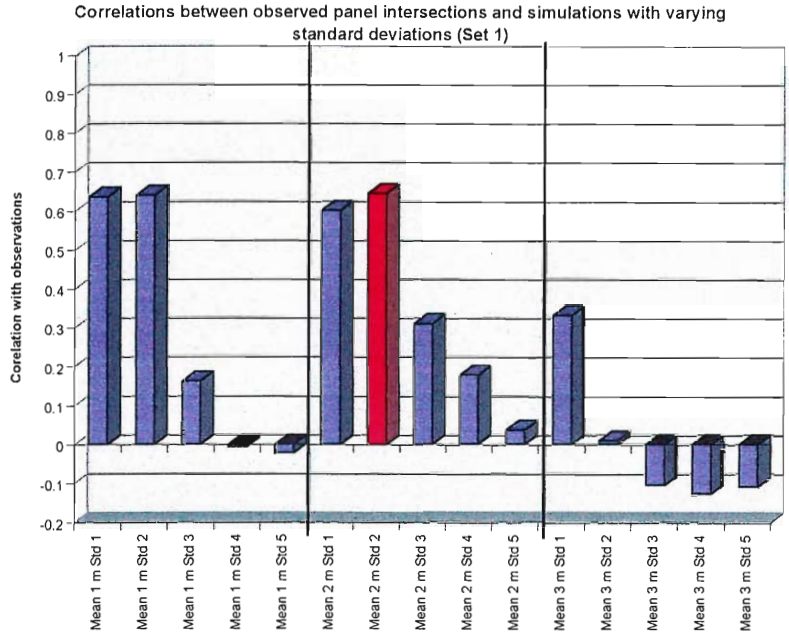

Figure 3-6. *Correlation between observed and simulated traces for orientation set 1 (NE-trending). To optimise the size analysis, a simulated size distribution in the estimated mean window is varied in standard deviation. The best fit estimation is observed for lognormally distributed fracture sizes of mean sizes 1-3 m with a standard deviation of 1-2 m.*

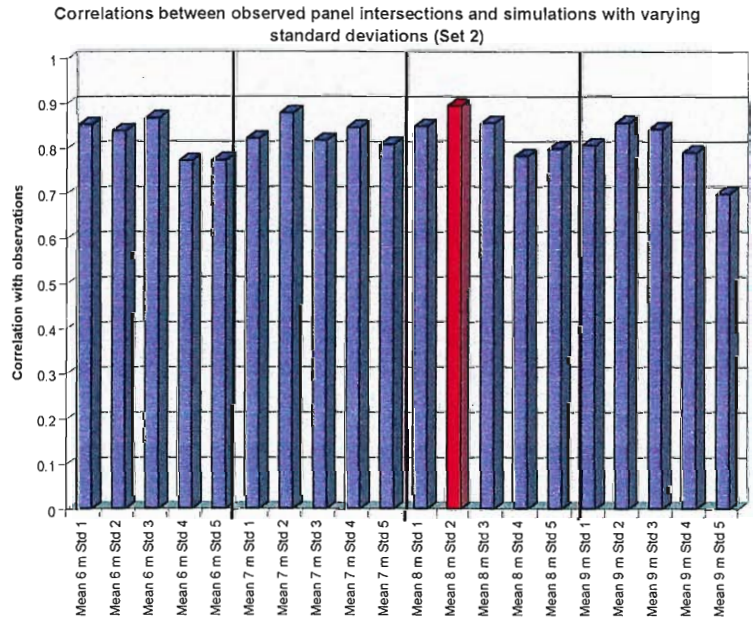

Figure 3-7. *Set 2 (NW-trending) correlation between observed and simulated traces in the mean size interval 6 to 9 m. The standard deviation is varied between 1 and 5. The best fit estimation is observed for lognormally distributed fractures of mean sizes of 5 to 9 m with a standard deviation of 2.*

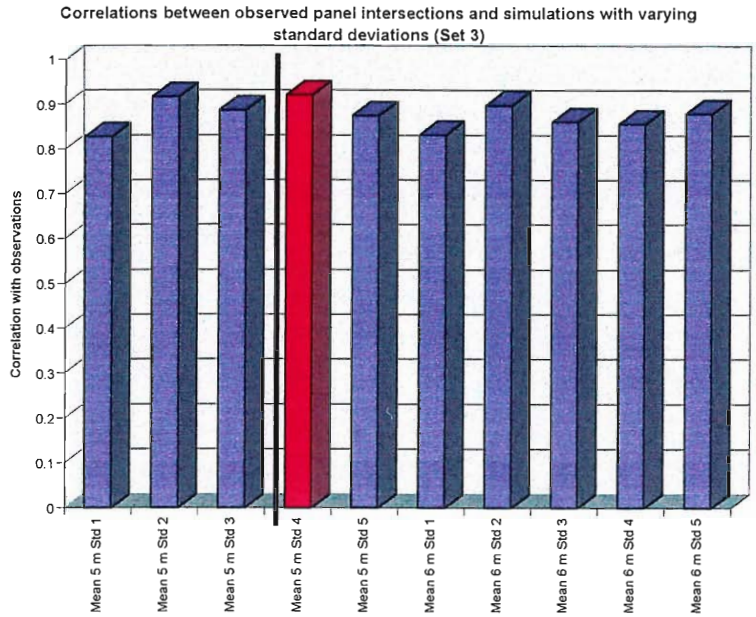

Figure 3-8. *Set 3 (Subhorizontal). The correlation between observed and simulated traces in the mean size interval 5 to 6 m (lognormal distribution) reveal that one cannot make more exact statements than the first estimate of a best fit estimate of mean size 4 to 7 m. A variation in standard deviation makes little difference.*

The second method Hermanson et al. (1997) used works similar to method 1 in all aspects except that traces are not converted to panel intersections. Instead the complete trace length distribution is used to estimate size. The best fit size distribution is estimated by comparing trace length statistics from observations and simulations. Both types of raw data have been used in this size analysis, i.e. SICADA data set and VBB Viak data set.

Hermanson et al. (1997) used a wide range of different possible lognormal fracture size distributions that resulted in a range of possible mean sizes. Examples of results are shown for fracture Set 1 in Figure 3-9 and Figure 3-10 for SICADA data. The best estimates are plotted in the cumulative density function (CDF) in Figure 3-9. If the standard deviation is increased more small and large fractures will be produced, i.e. the slope of the graphs in Figure 3-9 will be less steep. Figure 3-10 illustrates how well each of these estimates mimic the observed CDF for all different classes. Trend lines are inserted to show if the simulated traces tend to over or under-replicate traces. Ideally, the trend line should be located close to 0 (=little deviation) and have a slope of 0 (=no trend).

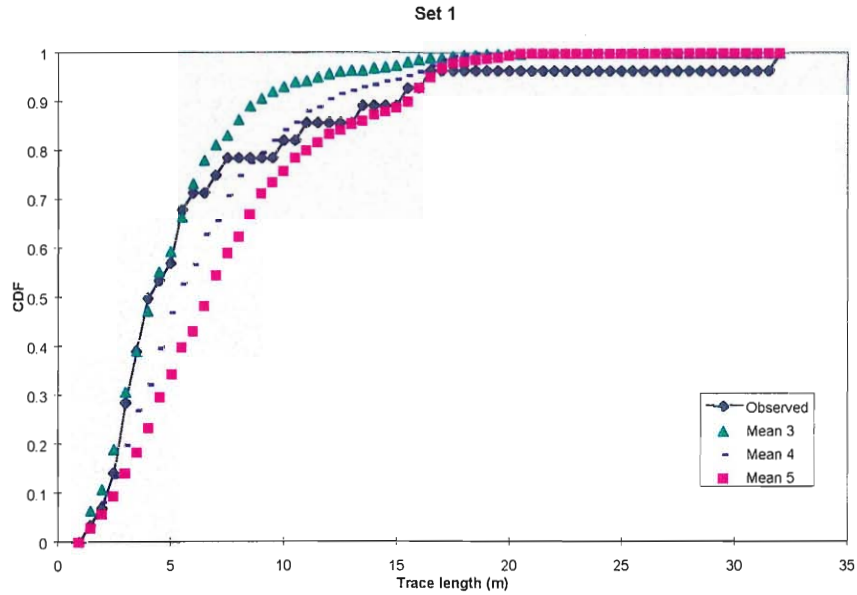

Figure 3-9. *CDF of observed trace lengths (blue line) and of the best fit simulated trace lengths for Set 1. The analysis suggests that a lognormal fracture size distribution with mean values around 3 to 5 m produces traces that fit well with the observed trace lengths.*

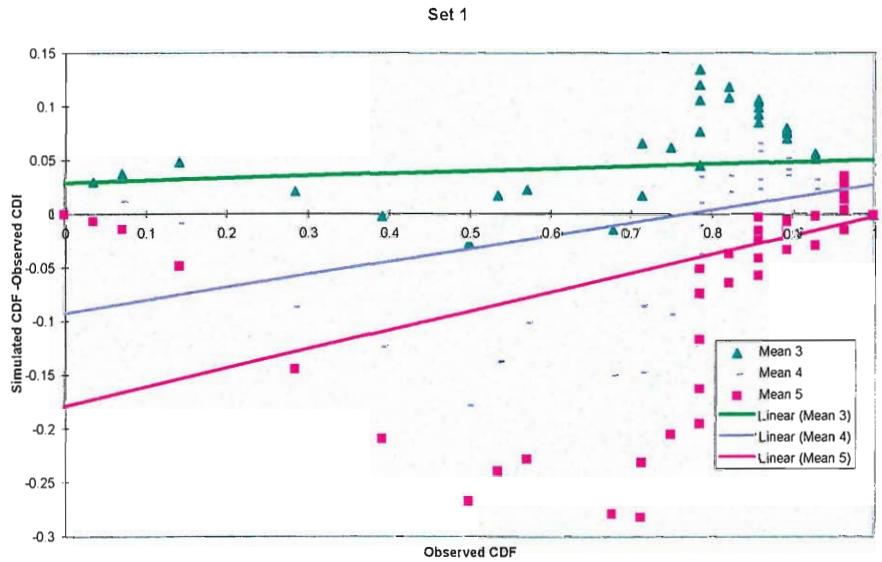

Figure 3-10. *Observed CDF plotted against the difference between Simulated CDF and Observed CDF. This plot illustrates how well the simulated trace lengths mimic the observed. Trend lines show if the simulations tend to divert from the observed CDF.*

Method 2 using the VBB Viak data set still reflects a similar range of lognormal fracture sizes although the VBB Viak data set has on average a larger trace length mean value than the SICADA data set. The size analysis is performed the same way for this

data as for the SICADA data set. Examples of CDF plots from set one are given in Figure 3-11 and Figure 3-12.

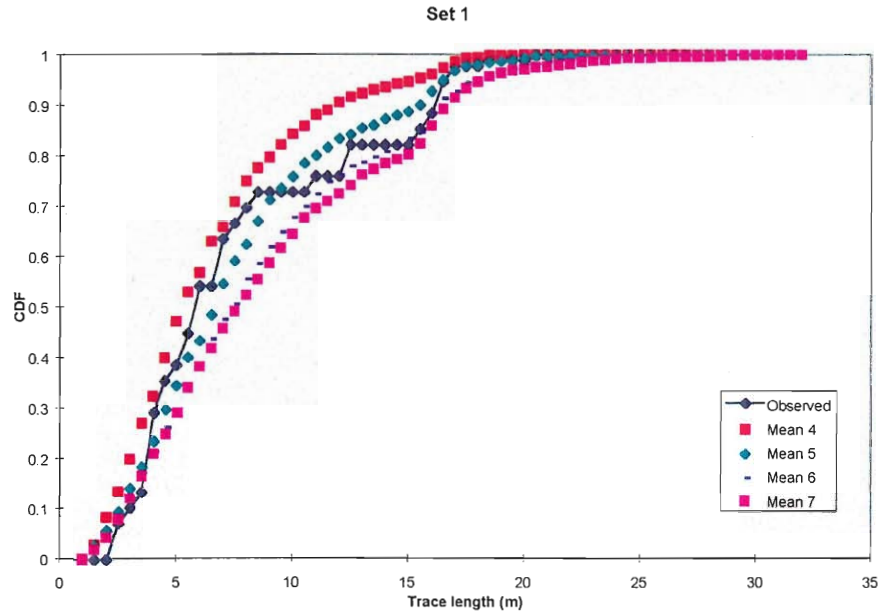

Figure 3-11. *CDF of observed and simulated traces using the VBB Viak data set. The best lognormal size distribution estimates range from mean 5 to 7 m.*

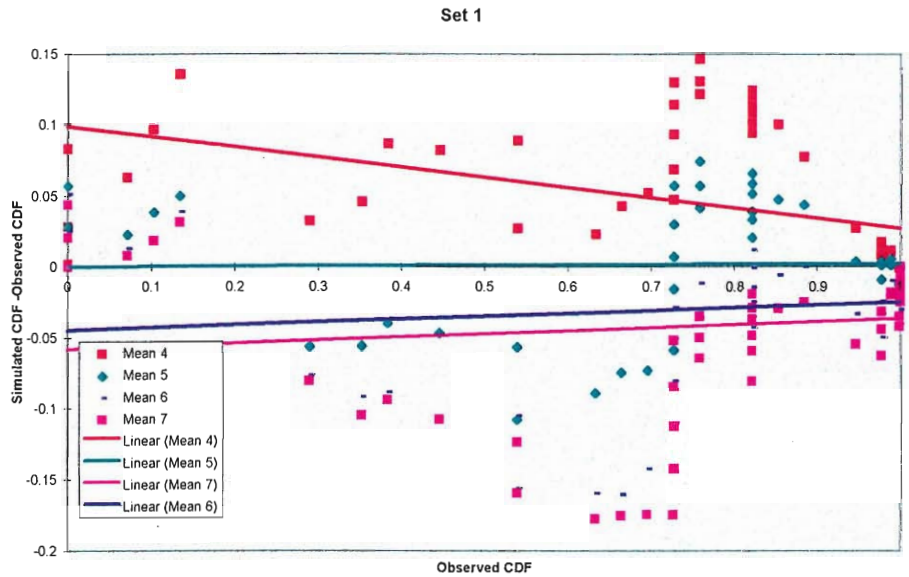

Figure 3-12. *Observed CDF plotted against the difference between Simulated CDF and Observed CDF. Results show little difference between observed traces and traces from simulated lognormal mean size distributions with means ranging from 4 to 7 m.*

The conclusions of estimates of fracture size from Hermanson et al. (1997) is shown in

Table 3-3. Size estimates are missing in the Prototype repository data and have therefore been deduced from this analysis without any further analysis.

Table 3-3. Estimates of fracture radius using two methods and two different data sets

		Method 1	Method 2	
		after La Pointe et al. (1993)	VBB Viak 3D data set	SICADA data set
Oct -97	Set 1	mean 2-3	mean 4-7	mean 3-5
	Set 2	mean 5-9	mean 4-6	mean 4-6
	Set 3	mean 4-7	mean 3-5	mean 2-4
TBM data 96	All	mean 6 std 3 (from Follin & Hermanson 1997)	mean 4-5	mean 3-5

3.3.3 Conductive fracture frequency, intensity and transmissivity distribution.

A numerical aspect of discrete fracture network modelling is the use of a transmissivity threshold to decrease the number of fractures in the model. This is justified by the argument that most of the fractures recorded in the drill cores at Äspö are not water-bearing and are thus of little use in a network model. Figure 3-13 below shows the complete set of mapped fractures in the central part of the TRUE Block Scale volume. The average total fracture frequency varies between 1.1 to 4.1 fractures per meter in the different boreholes in the TRUE Block Scale volume, c.f. Figure 3-13.

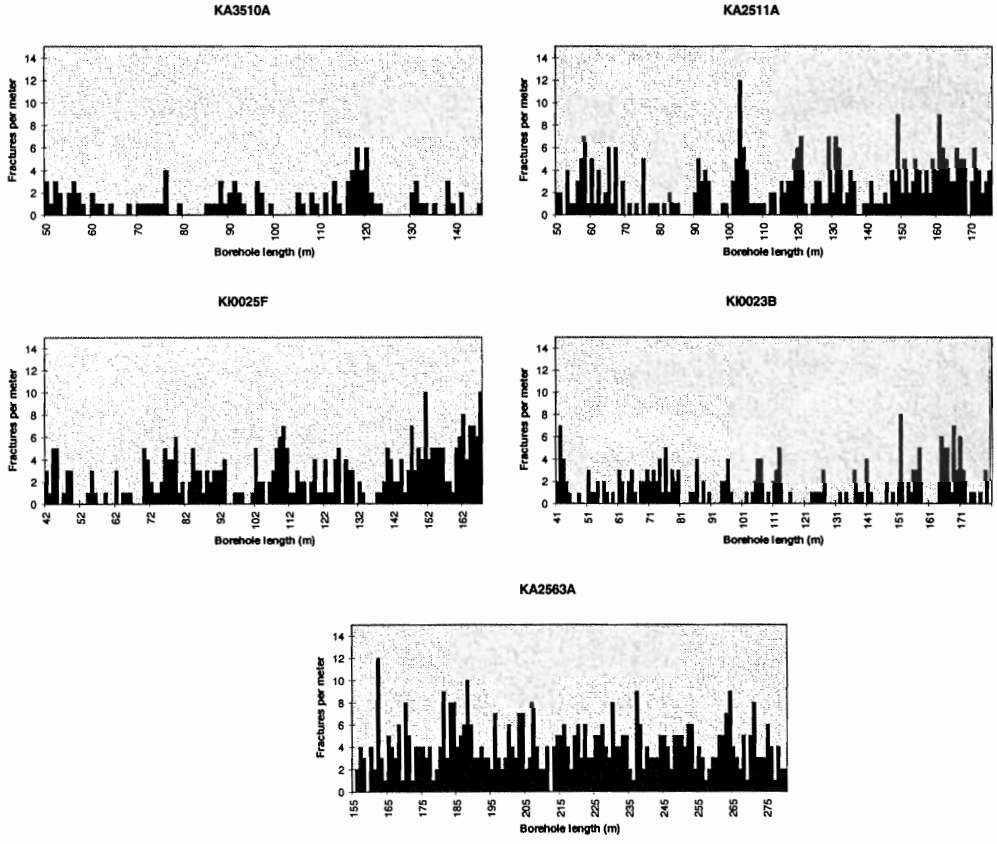

Figure 3-13. *Total fracture frequency in the central part of the TRUE Block Scale volume. The fracture frequency varies greatly along as well as between the*

boreholes. The average fracture frequency in the boreholes = $\bar{\lambda}_{KA3510A}$: $\bar{\lambda}_{KA2511A}$: $\bar{\lambda}_{KI0025F}$: $\bar{\lambda}_{KI0023B}$: $\bar{\lambda}_{KA2563A}$ *=1.1:2.6:2.6:1.5:4.1 fractures per m.*

For hydraulic flow simulations in a network it is preferred to simulate only a network of conductive fractures, i.e. skipping all the excess fracturing. This network can be estimated from the conductive fracture frequency, λ_c, i.e. fractures that take substantial part in the flow. Below follows a short explanation of how Follin and Wei (1997) uses detailed flow logs from the boreholes to quantify the conductive fracture frequency, λ_c, transmissivity distribution and finally conductive fracture intensity, P_{32c}.

Transmissivity in the TRUE Block Scale project is estimated in 5 m sections in the central part of the experimental volume, c.f. Figure 3-14. The idea is to relate the transmissivity in one section, T_{sec}, to λ_c. This is not a trivial task as there can exist more than one conductive fracture per section.

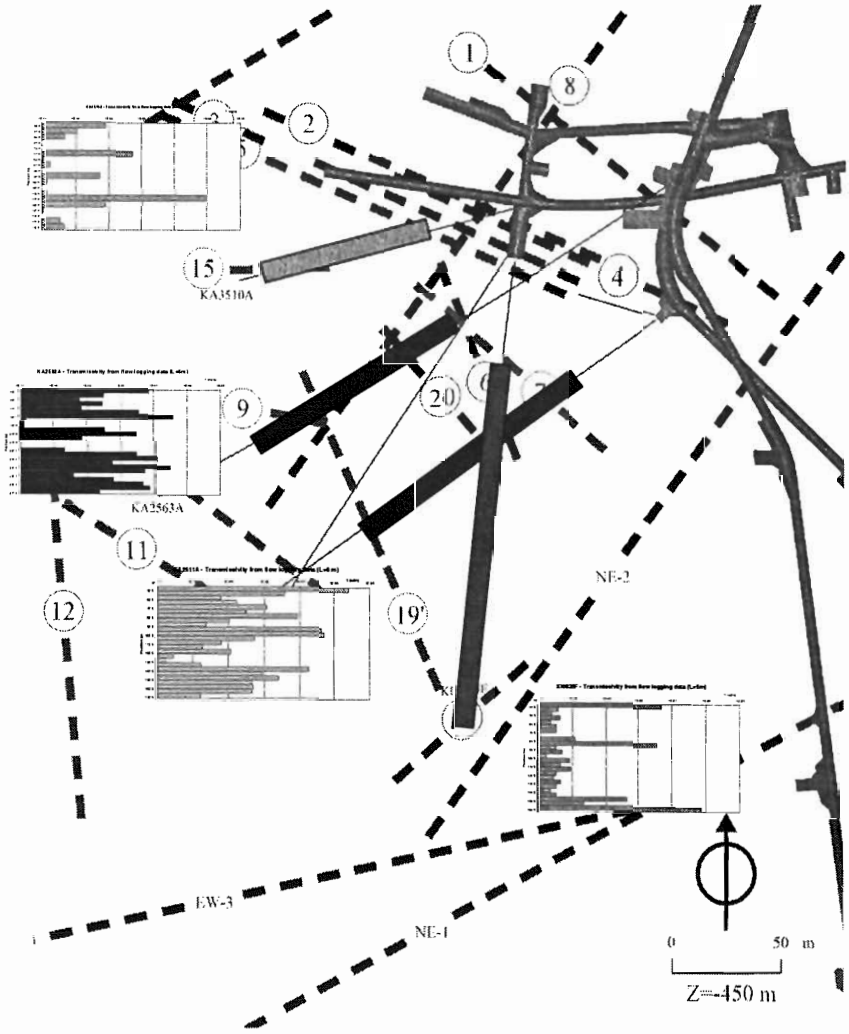

Figure 3-14. *Geographic extents of the conducted flowlogging measurements in the TRUE Block Scale volume. The histograms show interpreted transmissivity values. For more detailed histograms see Appendix C.*

Follin and Wei (1997) uses the OxFilet module to estimate the transmissivity distribution of the background fracturing for a given λ_c. This method assumes that the

net transmissivity of a test section is equal to the sum of the transmissivities of the conductive fractures that intersect that test section. This non-uniqueness requires that λ_c is known a priori. An upper estimate of λ_c is equal to the total fracture frequency in the most fractured borehole KA2563A, ca 4.1 fractures per meter. Follin et al (1998) explains that to obtain a good match in the OxFilet analysis λ_c can vary between 0.2-0.3 in boreholes with few transmissive sections. On the other hand, λ_c needs to be as high as 2 to obtain a good match in boreholes with many transmissive sections

In this report λ_c was chosen to be as small as possible to decrease the number of simulated fractures in the model as far as possible for numerical computational reasons and therefore λ_c is chosen from the lower end of the estimated population.

In the simulations of the Prototype repository we use the 5 m tests analysed by Follin and Wei (1997) with OxFilet, where λ_c equals 0.4 with a lognormal transmissivity distribution of $\log_{10}(T) \in N(-8.89,1.01)$. Recent material from the TRUE Block Scale borehole KI0023B shows that the chosen transmissivity distribution may be at least one order of magnitude larger than from the less transmissive boreholes in the TRUE Block Scale volume.

Table 3-4. OxFilet interpretation results for the TRUE Block Scale boreholes modified after Follin et al. (1997 and 1998).

Borehole	λ_c		μ_{logT}	σ_{logT}
KA2563A	0.4	**5 m tests**	-8.89	1.01
or	2	**5 m tests**	-11	1.7
KA2511A	2		-11	1.7
KI0025F	0.2-0.3		-11	1.7
KA3510A	0.2-0.3		-11	1.7

To implement the λ_c into a fracture network model it is necessary to convert this linear frequency to a volume intensity, P_{32c}. The conductive fracture frequency, λ_c, is a measure of "linear intensity", i.e., measured along a borehole or scanline and depends strongly on the orientation of the borehole as well as the orientation of the fracture population. For simulations with FracMan/MAFIC, it is much better to use the intensity measure P_{32c}, i.e. the conductive fracture area per unit volume of rock. This intensity measure is scale-invariant, i.e., independent of model size, fracture sizes, and boreholes lengths and orientations. The determination of P_{32c} from λ_c is accomplished by using the following procedure:

1. assume an initial guess of P_{32c}; and generate a fracture network using the given fracture orientation and size distributions,

2. sample the network with a borehole similar in orientation to the one where data has been collected, and calculate $\lambda_{c(initial)}$ for the initial P_{32c} ,

3. calculate the "true" P_{32c} corresponding to the "true" λ_c =0.4 as:
   $P_{32c} = 0.4 \times P_{32c(initial)} / \lambda_{c(initial)}$

Follin et al. (1997) shows that for the above given parameter data the total P_{32c} for the fracture network equals 0.7 m^2/m^3.

3.3.4 Spatial model

A spatial analysis of the trace maps from the TBM tunnel has been done by Follin & Hermanson (1996). The spatial model is estimated by analysing the pattern of fracturing along an outcrop such as the end of the TBM tunnel, c.f. Figure 3-15. The trace map is overlain by a grid and the number of traces within each grid cell is calculated. Figure 3-16 shows a plot of the probability density function of number of traces in each grid cell when changing the cell size. Simulated tracemaps are matched to the observed data until a 99% significance level is reached for the χ^2 –test. If then the box dimension (i.e. slope of the curve on a plot of no. of grid cells versus cell size) is close to 2 we have a Poisson distributed model. If the box dimension is larger than 2 the model needs to be more clustered and purely fractal if the box dimension is 3. The analysis indicates that a Poisson distributed model for the observed data is appropriate. For further explanations see Appendix A.

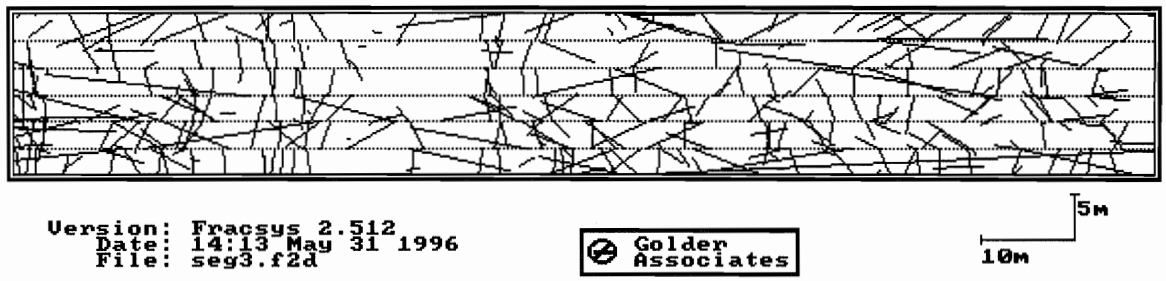

Centre line characteristics: L =122.03 m, Trend = 277.16, Plunge = -0.94
x = 1,984.84, y = 7,262.33, z = –447.768
P_{21} = 0.656 m/m^2

Figure 3-15. *Trace map over the last 120 m of the TBM tunnel.*

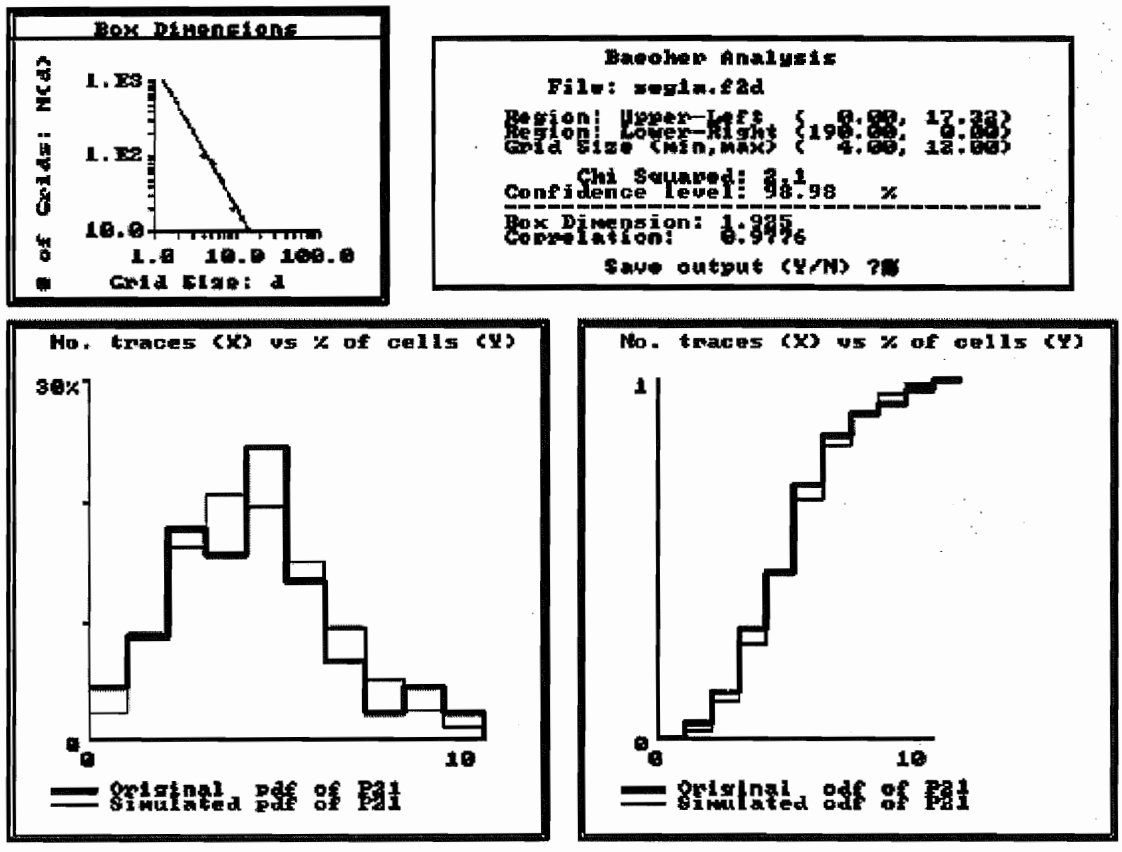

Figure 3-16. *A spatial analysis of the trace maps from the TBM suggests that a Poisson distributed spatial model with a homogeneous space filling may be appropriate*

4 DFN model set-up

Data from the 1st drilling campaign includes fracture frequency and borehole transmissivity information. This data together with data from other studies in the vicinity of the TBM tunnel is the basis for the DFN model.

4.1 Model geometry and location

To completely surround the Prototype part of the TBM tunnel and to include tunnels that are close enough to influence the flow field around the deposition holes, it is suitable to generate a model with the size of 150 x 100 x 100 m as visualised in Figure 3-1 and Figure 5-1. The centre point of the volume is located at (7271,1911,-448) in Äspö co-ordinates. A fracture network of this size requires substantial computer power to simulate flow in detail. With the above given DFN parameters and model size we look at a model with approximately 22000 fractures which contain more than 500 000 finite elements with 160 000 nodes in the finite element mesh. To perform simulations in this model we have used the finite element code MAFIC on a Digital Alpha 500 MHz with 1.3 GB of RAM.

4.2 Spatial assignment of fracture network

The following parameters need to be deduced from the available data from

1. Orientation distribution
2. Size distribution
3. Spatial fracture model
4. Conductive fracture intensity, P_{32c}
5. Transmissivity distribution

4.2.1 Orientation distribution

The orientation distribution is deduced from SICADA data of the TBM tunnel section 3480-3600. Since there is not a clear evidence for dividing the fractures into sets, the model uses a "bootstrapped" orientation distribution. Bootstrapped orientation means that simulated fracture orientation are generated exactly according to the observed distribution. This implies that the simulated population reflects exactly what has been measured in the field. This method is useful in our case as we initially think that fracture sets have similar properties. However, in one of the sensitivity analysis, described below, we have actually made use of fracture sets rather than bootstrapped fractures to test the sensitivity of steep and subhorizontal conductive fractures.

4.2.2 Size distribution

In Hermanson et al. (1997), see Table 3-2, the north-west trending set, set 2, is the most dominating in the TBM tunnel, section 3480-3600. In all 46% of the fractures are included in this set. This set is also the set that has the largest fractures. A mean radius of 6-9 m gives good correlation. The other two sets have good correlation for fractures with mean radius 2-3 m and 5-6 m. If all fractures are considered to have the same mean size, i.e. bootstrapped fracture distribution, the mean radius is 6 m (method 1), see Table 3-3.

The flow model only considers conductive fractures. The non-conductive fractures would, if included, only give rise to more nodes that do not add information to the solution. However, the background data do not contain any information of which fractures that are highly conductive or non conductive, but intuitively it is the small fractures that are less conductive. This implies that a larger mean radius should be used than given by method 1 in Table 3-3. To compensate for the loss of the small fractures, that occur when conductive fractures are simulated, a larger standard deviation is used.

Therefore we assume that the size of the conductive fractures should have a mean value of 9 m and a standard deviation of 5 m, which reflects the maximum values deduced by method 1.

4.2.3 Spatial fracture model

According to discussion in chapter 3.3.4 a poison distribution and enhanced Baecher model is used.

4.2.4 Conductive fracture intensity

In the pilot holes the fracture frequency, λ, is 0.48 fractures/m according to SICADA data. Follin and Wei (1997) show that if the fracture frequency is 0.43 m^{-1} then 87% of the fractures have a transmissivity greater than $1 \cdot 10^{-10}$ m^2/s. This implies that the conductive frequency, λ_c, is 0.42 m^{-1} ($0.48 \cdot 87\%$). A P_{32c} of 0.7 m^2/m^3 gives λ_c of 0.42 m^{-1}.

4.2.5 Transmissivity distribution

Follin and Wei (1997) suggested that the transmissivity could be described by a lognormal distribution with a $\log_{10}$ mean of -8.89 and $\log_{10}$ standard deviation of 1.01 for the 5 m test sections. Only the conductive fractures are modelled so the transmissivity distribution has to be truncated for low values. The lower truncation is $1 \cdot 10^{-10}$ m/s^2. No correction neither to size nor orientation is assumed.

4.3 Deterministic structures

Zone EW-1 from the site scale model by Rhén et al. (1997) has been implemented in the model. Only structure EW-1 from the TRUE Block Scale project is included and the transmissivity is $T = 1.7 \times 10^{-7} m^2/s$ according to (Rhén et al., 1997).

4.4 Boundary conditions

4.4.1 Outer boundaries

Specified head is applied to all of the outer boundaries. The heads have been derived from the site scale finite difference flow solution presented in Svensson (1997). The pressure from Svensson's model is converted to fresh water head according to:

$$H = Z + p_{US} / (\rho_w \cdot g)$$

where

- H = Fresh water head [m]
- Z = Current elevation in [m]
- p_{US} = Pressure from Svensson (1997) [Pa]
- ρ_w = density of fresh water [Kg/m^3]
- g = Constant of gravity [m/s^2]

To get a smooth head field from Svensson's discrete 25 m blocks, a 3D interpolation has been performed using the 6 nearest values.

4.4.2 Inner boundaries; tunnels, pilot holes and deposition holes

The tunnels included in the model are shown in Figure 3-1 and comprise segments from the last part of the TBM tunnel, the G-tunnel and the F- tunnel. The tunnels are implemented with a specified head boundary with atmospheric pressure to simulate the effect of open tunnels. Inflow from the F-tunnel is used for calibration and sensitivity study of the model.

When inflow was measured in the 1st drill campaign pilot holes a packer with a pipe system was put on top of each borehole so that the opening of the borehole was approximately 1.4 m above the tunnel floor according to Gentzschein (personal communication, 1998). This implies that the pilot holes have to be implemented in a similar manner not to overestimate the possible inflow. Measurements are also performed in one hole at a time, where all other holes are closed. The pilot holes are implemented in the model with a specified head boundary condition corresponding to a 1.4 m high pillar of water above the tunnel floor. When simulating inflow to these boreholes, inflow is calculated with only one borehole open at a time.

The deposition holes are implemented in the same manner as the tunnels as they are open and presumably not filled with water when inflow is measured.

4.5 Summary of DFN model parameters

In Table 4-1 below is a summary of the parameters that is used in the DFN model shown.

Table 4-1. Summary of used parameters for the DFN model.

Parameter	Used data	Data from	Reference
Orientation	bootstrapped and by fracture sets as defined in Table 3-2	TRUE Block Scale	Hermanson et al (1997)
Size	$\log_{10}$ mean 9 std 5	TRUE Block Scale	Hermanson et al (1997)
Location model	Enhanced Baecher		
Conductive intensity, P_{32c}	0.7 from 5m test	TRUE Block Scale and pilot holes	Follin et al (1997)
Transmissivity distribution	$\log_{10}(T) \in N(-8.89,1.01)$ truncated at $1 \cdot 10^{-10}$ m^2/s	TRUE Block Scale	Follin et al (1997)
Model size	150 x 100 x 100 m		
Centre point in Äspö Co-ordinates	North = 7271 m East = 1911 m Z = -448 m		
Boundary conditions	Specified head boundary	site scale model	Svensson (1997)
Inner boundaries	Tunnels as head simulating atmospheric pressure p=0. Boreholes no flow or head according to performed tests	Performed tests	Gentzschein (personal communication 1998)

5 Model sensitivity study and calibration

5.1 Base case model

The base case model is based on DFN parameters from Table 4-1and the deterministic structure EW-1 given by Rhén et al. (1997). Figure 5-1 show 10 % of the generated fractures in the base case model. The model contains the last section of the TBM tunnel, F-tunnel, G-tunnel and J-tunnel. The generated stochastic fracture network is then sampled with the pilot holes from the 1st drilling campaign. Although the fracture statistics from the 1st drill campaign has been used to determine the DFN parameters it is useful to control that the simulated parameters are correct. Figure 5-2 shows the expected good correlation between simulated and observed fracture frequency.

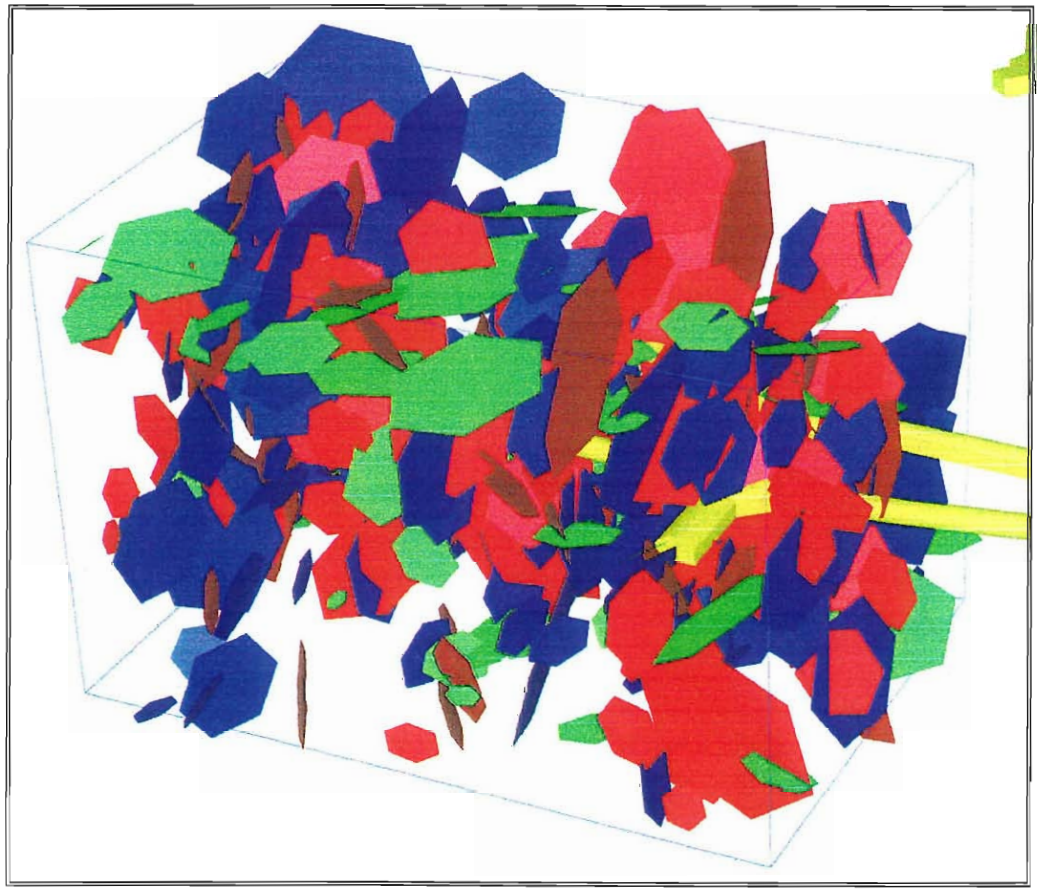

Figure 5-1. *Visualisation of 10% of the fractures in the model and the location of the model block.*

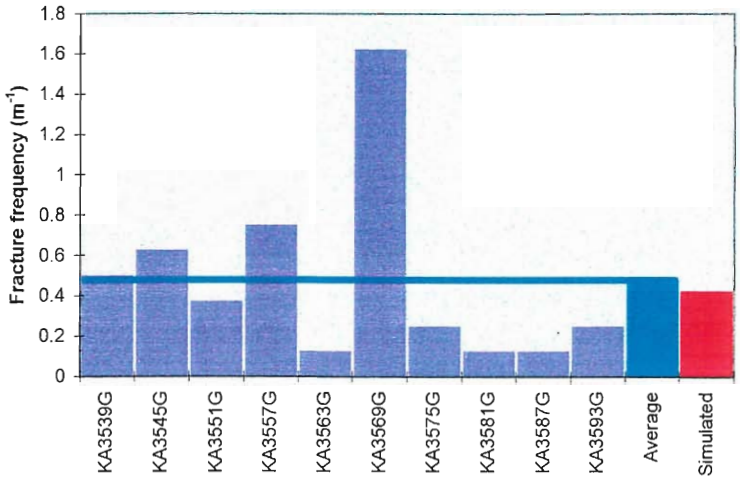

Figure 5-2. *Conductive fracture frequency in the simulated pilot holes compared to all measured fractures. The blue line represents the average observed total fracture frequency.*

Ten stochastic fracture network realisations are simulated based on the above given DFN parameters and each realisation is meshed and fed into MAFIC. Flow simulations are performed with one pilot hole open at a time, i.e. ten flow simulations in each stochastic network realisation, which in total sums up to one hundred flow simulations in the base case model. A summary of the results is shown in Figure 5-3. Inflow into the tunnels is simulated without the presence of any pilot holes in the model to simulate the real situation when flow was recorded in the weirs. Since there is no available data for the inflow to the G-tunnel the observed flow is estimate by having the same inflow per meter as the F-tunnel, where observed data exists. The reason for doing an extrapolation is that only a small part of the F-tunnel is modelled and that this part is close to the boundary. The tunnel measurements are fairly well matched with simulated results. However, inflow to the pilot holes in the floor of the tunnel is overestimated approximately two times.

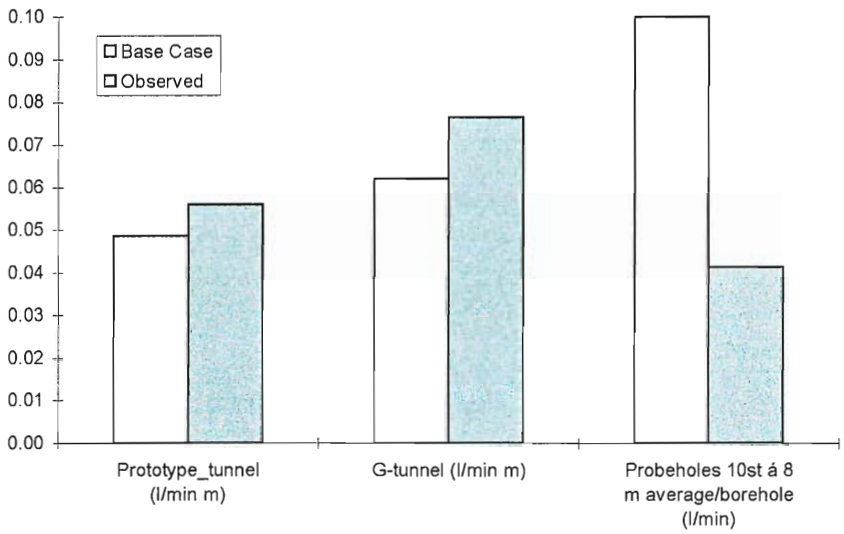

Figure 5-3. *Results of the flow simulation with the uncalibrated base case model. The flow in the G-tunnel is assumed to be the same as observed in the F-tunnel.*

The calculated net inflow over the outer boundaries in the base case model with implemented pilot holes sums up to an average of 13.7 l/min. If we add the deposition holes to the base case model we increase the net inflow over the outer boundaries to an average of 14 l/min. This increase is considered natural as a larger sink is created with the deposition holes than without.

5.2 Impact of outer boundary conditions on the simulated inflow to the tunnels, probe and deposition holes

To evaluate how the boundary conditions influence the flow simulations we have used the base case model but changed the outer boundary conditions to zero head gradient. I.e. the specified heads extracted from Svensson (1997) are replaced with a constant head of zero. This influences the inflow to the model in several ways as can be seen in Figure 5-4. A zero head gradient decreases inflow to the prototype tunnel and increases inflow to other tunnels and to the deposition and pilot holes. However, the relative change is less than 8% and show that the outer boundary conditions have a limited effect on the flow field around the Prototype repository. It also confirms that the chosen simulation domain is adequate in size.

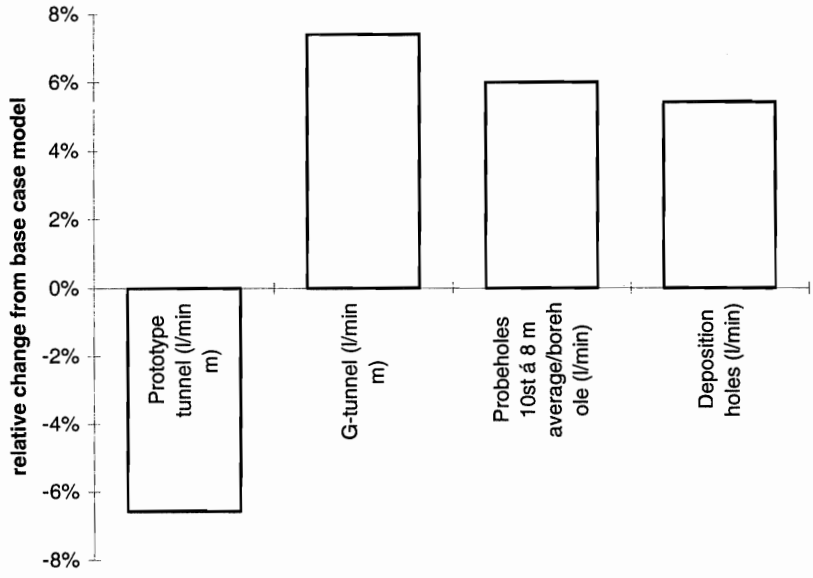

Figure 5-4. *Relative change of inflow as compared to the base case model to the tunnels, probe and deposition holes. The net inflow over the outer boundaries shows a relative increase of 8%.*

5.3 Effect of the nearby tunnel system in the model

The sensitivity of the model is tested by removing the nearby tunnel system. The G-tunnel, F-tunnel and J-tunnel are removed from the model. Flow simulations are performed and inflow to the Prototype tunnel and the deposition holes are calculated as well as the flow over the outer boundaries. Inflow to the deposition holes is severely affected by the distance to the removed tunnel sections as can be seen in Figure 5-5. The effects of the nearby tunnels are quite substantial as inflow to the main tunnel and to the closest deposition hole increases with 25% and 15% respectively. The relative increase in inflow to the deposition holes becomes less pronounced with distance to the removed tunnels. The inflow to the tunnel and the most eastern deposition hole is, in absolute numbers, on average 0.06 l/(min m) and 0.23 l/min respectively.

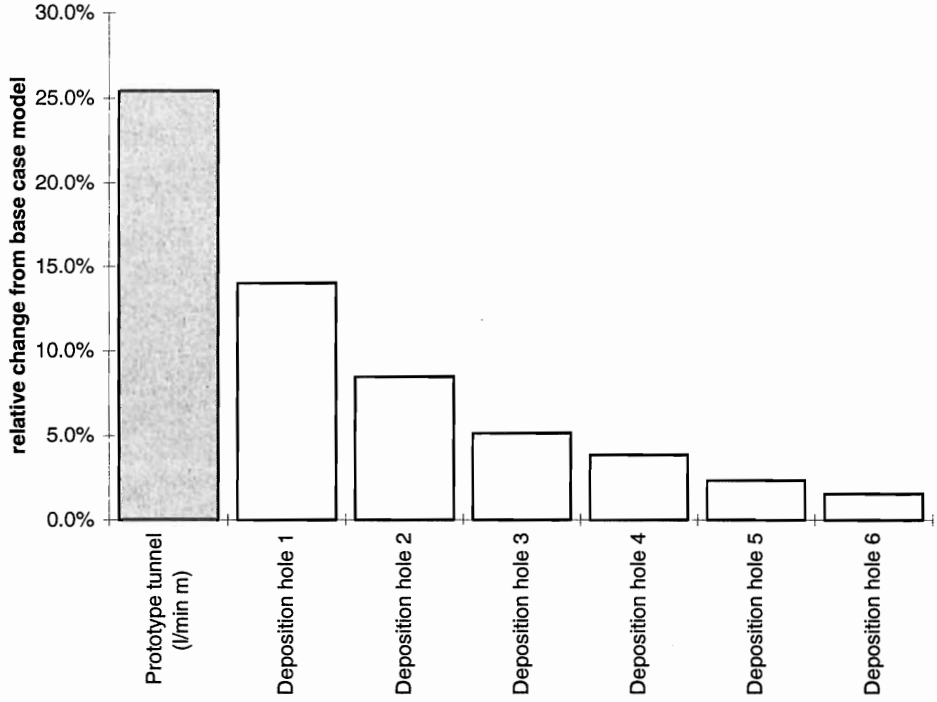

Figure 5-5. *Effect of removing the nearby tunnel system as relative change of inflow calculated for the base case model.*

5.4 Correlation of transmissivity and size of fractures

It is often observed how long faults in the Äspö HRL are highly water conducting in comparison to smaller fractures. This sounds reasonable as longer fractures have gone through a more intense deformation with a higher probability of having a larger aperture and size. They are also connected to more fractures than smaller ones. The idea of large conductors also sounds attractive as that would limit the need for generating so many fractures in the model.

The hypothesis with more conductive fractures is quickly tested by correlating T to size by maintaining the same transmissivity distribution as if T was set randomly to the fractures. The largest transmissivity from the distribution is then assigned to the largest fracture. The fracture intensity, orientation and size distribution are all maintained. Figure 5-6 shows that the simulated inflow is considerably overestimated as compared to the base case model. This effect can be explained by the fact that the assigned T-distribution is based on a conductive network with no coupling to size. The results show that if the assumption of coupled T and size is to be used one must take fracture size into account when estimating the T distribution. Observations of fracture traces can also influence these results. Follin and Hermanson (1996) describes that the observed traces from the TBM tunnel are measured with a lower truncation of 1 m. This has a major influence to the assignment of transmissivities to the smallest fractures as the T distribution is lognormal.

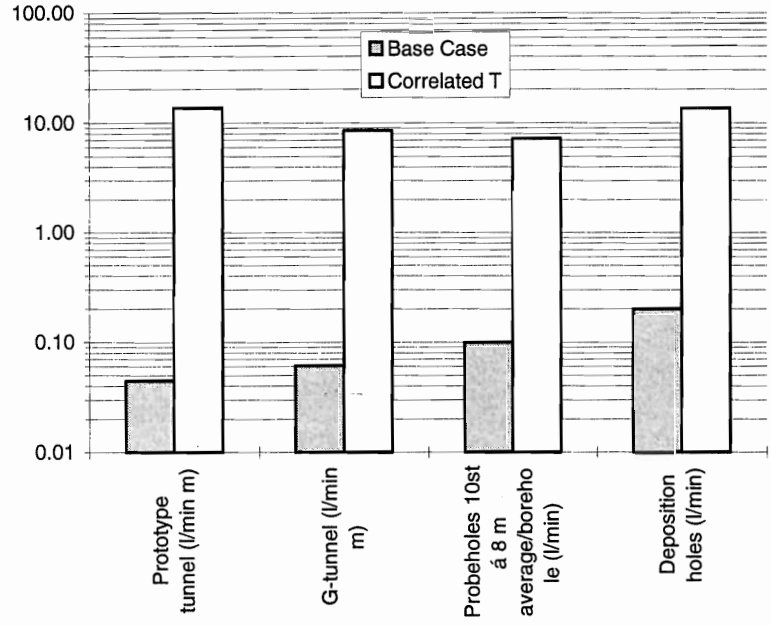

Figure 5-6. *The effect of correlating T to fracture size overestimates inflow. The main explanation is that the fracture network is already truncated by the approach of simulating a truncated set of conductive fractures.*

5.5 Effect of simulating only steep conductive fractures

Observations in the Äspö HRL indicate that inflow occurs mainly from steep rather than sub-horizontal fractures and fracture zones (Rhén et al. 1997). There exist indications that sub-horizontal fractures act as a more or less non-conductive fracture set in the TRUE Block Scale volume (Hermanson et al., 1997). The hypothesis of steep conductors is tested by removing the sub-horizontal fractures in the simulated fracture network. All other parameters are identical to the base case model.

Data for the fracture set separation is derived from the TRUE Block Scale project and is given in Table 3-2. The summary of these three fracture sets corresponds to generating fractures according to the bootstrapped concept used in the base case model. In this variant case is the sub-horizontal fracture set, Set 3, simulated as a non-conductive set to test the effect of having only steep conductive fractures in the block. The sub-horizontal fractures are removed from the network but the fracture intensity, P_{32}, is kept to maintain the correct conductive fracture intensity and size distribution. Transmissivity is assigned to the remaining steep fractures according to the derived transmissivity distribution.

The results of simulating only steep conductive fractures compared to the base case show that sub-horizontal fractures have a small impact on the tunnel inflow but becomes more significant in the inflow to probe and deposition holes. This is a desirable effect as the simulations of the base case model overestimate inflow to the vertical 8 m pilot holes. The reason being that there is a higher probability that sub-horizontal fractures intersect the pilot holes than steep fractures, and when all sets are equally conductive, inflow is subsequently overestimated in vertical boreholes. This effect will be somewhat lower in a larger hole, such as the deposition holes, as the probability that such a large hole will intersect a steep fracture increases relative to the pilot holes.

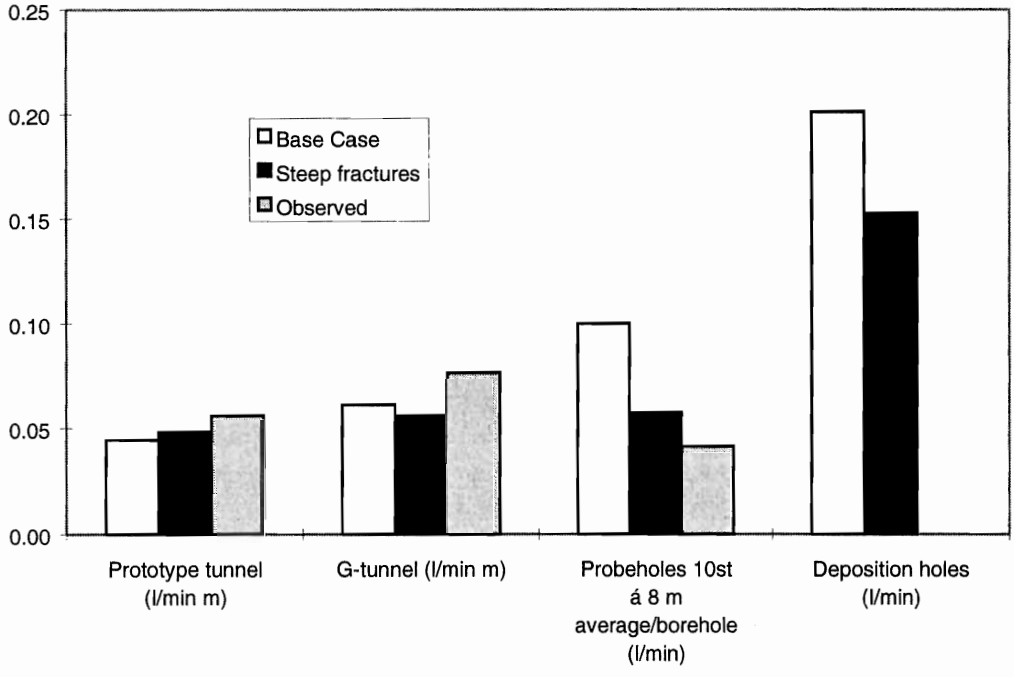

Figure 5-7. *Effect of inflow to the tunnel, probe and deposition holes simulating only steep conductive fractures.*

6 The 2nd drill campaign and the planned deposition holes

The 2nd drill campaign consists of twelve vertical pilot holes, ten of 12 m length and two of 8 m length. They are situated in the floor of the TBM tunnel at unknown places. The actual location of the boreholes has no effect on the simulated result of fracture characteristics. However, it may influence the inflow through the nearby tunnels. In this simulation inflow has been calculated as if all boreholes where within the limit of the planned deposition holes. The pilot holes are implemented with a 1.45 m high collar above the tunnel floor, as indicated by personal communication with Gentzschein (1998).

The predictions of the fracture statistics in the pilot holes of the 2nd drill campaign are made with the same DFN model parameters as given in the base case model in

Table 3-3.

6.1 Predictions of fracture statistics of the 2nd drill campaign and deposition holes

The statistics are based on ten stochastic realisations of the fracture network. Ten pilot holes with the length of 12 m and two with the length of 8 m are sampled in each realisation.

Around 40 fractures intersect the complete set of pilot holes per realisation. Conductive fracture frequency is predicted to be on average 0.34 fractures per meter. Fracture orientations are mainly gently dipping fractures with a tendency of a NW trending steeper set, c.f. Figure 6-1.

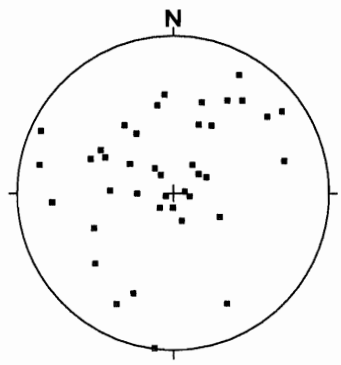

Figure 6-1. *Conductive fracture orientations in the pilot holes of the 2nd drill campaign from one realisation.*

The fracture orientations of the deposition holes are essentially the same as in the pilot holes. However, the deposition holes are big enough to record fracture traces on the walls of the hole. Figure 6-2 shows four examples of fracture traces on the walls of a deposition hole with a typical array of fractures. Sub-horizontal traces are common,

although slightly overemphasised in the pictures as they are not exactly to scale. The average trace length per area unit, P_{21c} equals 0.4 m/m^2. Remember that this tracemap only covers fractures though to be conductive. A true trace map of the rock will contain many more and shorter traces of "dry" fractures.

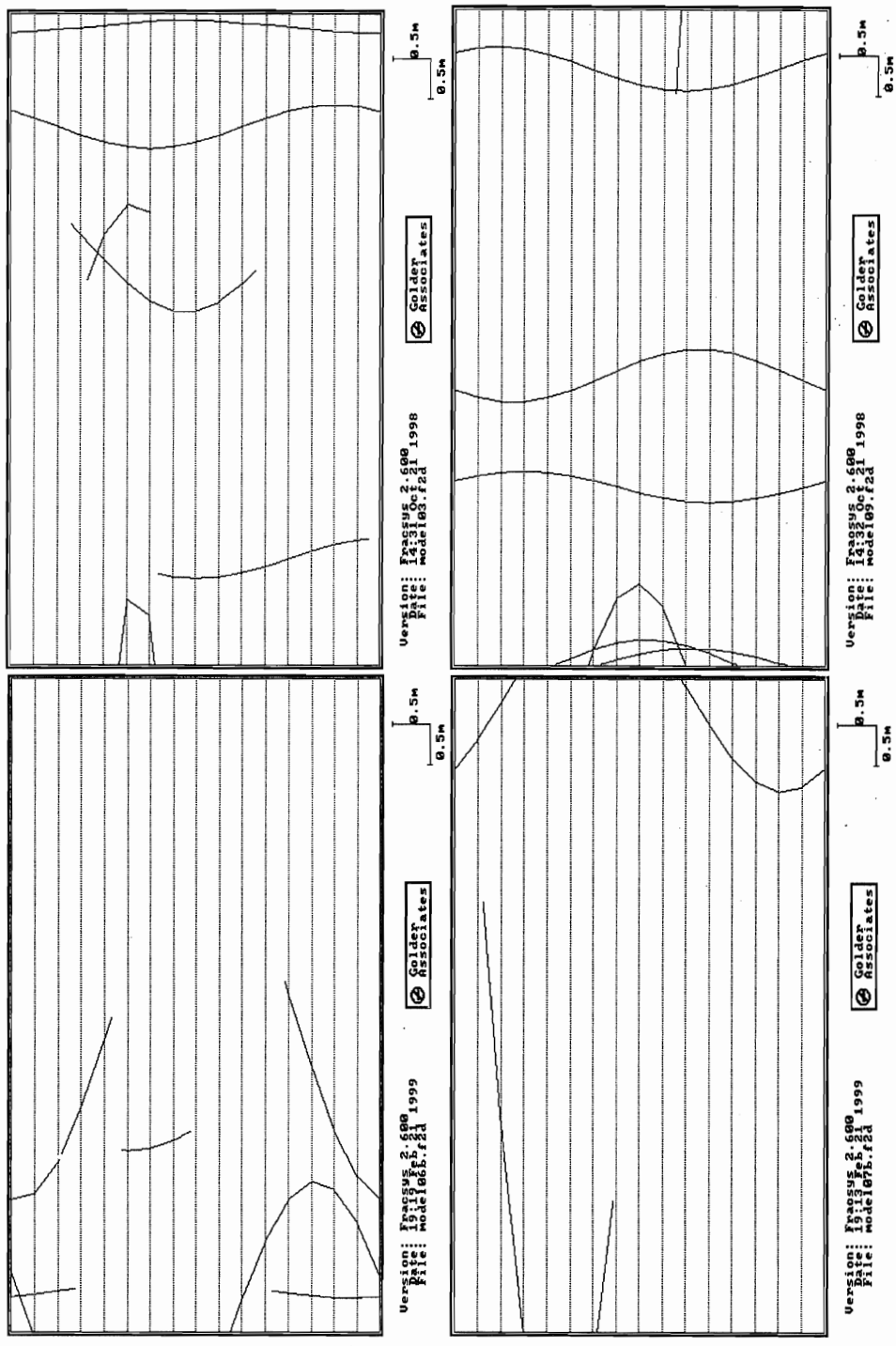

Figure 6-2. *Fracture traces of conductive fractures from four realisations of a deposition hole. The average trace length per area unit, P_{21c} equals 0.4 m/m^2.*

6.2 Predictions of inflow to the 2nd drill campaign and deposition holes

Inflow predictions are made with an optimised table of DFN parameters, c.f. Table 6-1. It is argued that most of the conductive fractures are steep with reference to the overestimated inflow to pilot holes of the 1st drill campaign in the base case model. The outer boundary conditions are derived from Svensson (1997) and are considered favourable to a specified head boundary as Svensson's solution indicates a weak gradient towards the central part of the HRL due to the presence of the tunnel system. Tunnels and deposition holes are implemented as open tunnels, i.e. as head boundaries with atmospheric pressure.

The pilot holes of the 2nd drill campaign are implemented one at a time to simulate a real situation where each borehole is closed after drilling. The deposition holes are implemented all at once and inflow is calculated in all holes simultaneously. This approach will probably underestimate inflow slightly as the real drilling of the deposition holes will take place one after another, with inflow measurements in each hole and where finally all holes are left open.

The predicted inflow to the pilot holes of the 2nd drill campaign is on average 0.07 l/min, c.f. Figure 6-3. The average inflow to the deposition holes is estimated to 0.15 l/min, i.e. approximately the double amount of inflow as into the pilot holes.

Table 6-1. Calibrated DFN parameters

Parameter		Data from	Reference
Orientation	conductive fracture sets as explained in chapter 5.5	TRUE Block Scale	Hermanson et al. (1997)
Size	$\log_{10}$, mean 9 std 5	TRUE Block Scale	Hermanson et al. (1997)
Conductive intensity, P_{32c}	0.7	TRUE Block Scale	Follin et al. (1997)
Transmissivity distribution	$\log_{10}(T) \in N(-8.89,1.01)$	TRUE Block Scale (5 m tests)	Follin et al. (1997)
Model size	150 x 100 x 100 m		
Boundary conditions	Constant head boundary	site scale model	Svensson (1997)
Inner boundaries	Tunnels and boreholes as head boundary, p=0		

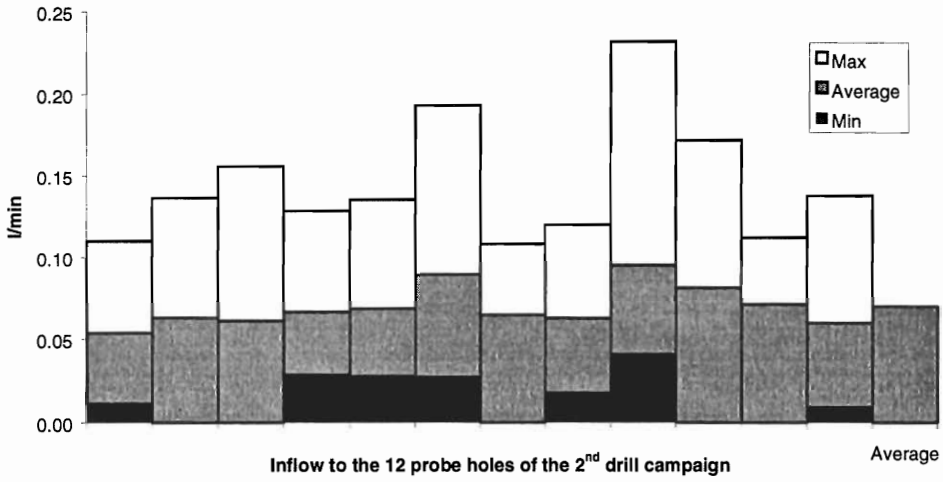

Figure 6-3. *Predicted inflow to the pilot holes of the 2nd drill campaign, min, average and max value from 10 realisations.*

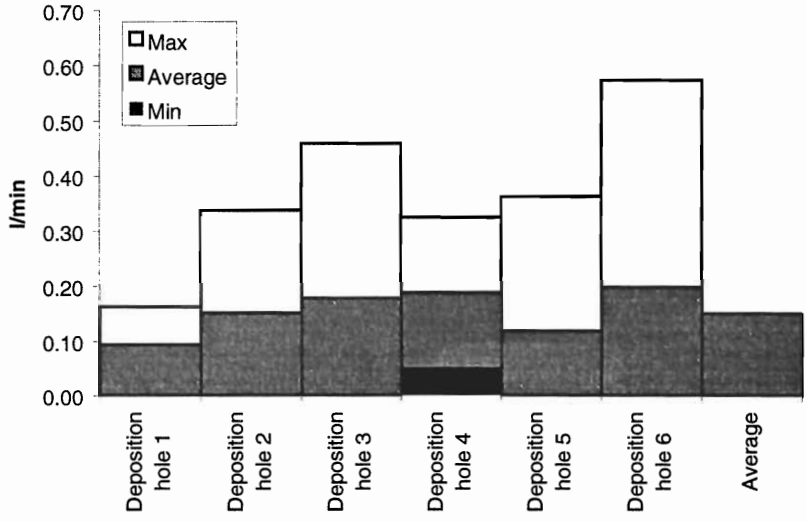

Figure 6-4. *Predicted inflow to the deposition holes, min, average and max values from 10 realisations.*

7 Conclusions and limitations

The limitations when simulating flow in fractured crystalline rock are of course great but can be minimised by using adequate data from the rock mass of interest. In this exercise we have used input data based on rather generic fracture data for the purpose of mimicking a real future situation when no detailed information of the rock mass exists.

The outer boundary conditions are derived from a large more generic model in lack of better information. However, the sensitivity study shows that the model size of the Prototype DFN model seems large enough to accommodate changes in the outer boundary conditions with limited change in flow conditions around the deposition holes. The effect of inner boundary conditions is larger. We do not know the effect of having a larger part of the Äspö HRL tunnel spiral within the model volume. But by removing the currently implemented tunnel system inflow conditions to the deposition holes change by more than 10% and the Prototype tunnel inflow by more than 20%.

The fracture network parameters are based on a rock volume next to the Prototype repository volume and should not deviate much from what can be seen in the TBM tunnel. However, the estimation of the conductive fracture intensity in the block is based on rather large packer tests (5m) and may significantly affect the properties of the DFN model. Follin et al (1997) show that P_{10c} could change from 0.4-2 m^{-1} by using different transmissivity distributions. In this model we have chosen to use the T distribution that minimises the amount of simulated fractures in order to be able to simulate as large model domain as possible.

Correlating size to high transmissive structures needs further understanding of the distribution of large waterbearing features in the rock mass. It is not possible to simulate based on the current understanding of fracture size and transmissivity distribution.

Structural geological interpretation of the conductive fracture network at Äspö has a considerable effect on the results of the simulations. This study shows that the major flow paths of the network can be explained by using only steep conductive fractures and considering sub-horizontal fractures as being "dry". The final DFN simulation also shows that if only steep conductive fractures are considered, inflow can be calibrated to both inflow in boreholes and into tunnels without using skin effects on the tunnel surface.

8 References

Dershowitz, W., Thomas, A. and R. Busse (1996) Discrete fracture network analysis in support of the Äspö Tracer Retention Understanding Experiment (TRUE-1), SKB ICR 96-05, Swedish Nuclear Fuel and Waste Management Company, Stockholm.

Follin, S, Hermanson, J., 1996. A discrete fracture network model of the Äspö TBM tunnel rock mass. Arbetsrapport AR D-97-001. Swedish Nuclear Fuel and Waste Management Company.

Follin, S., Wei, L., 1997. Input data for discrete feature network modelling of the TRUE Block Scale site. Part 2- Hydraulic analysis of the flow meter logging in borehole KA2563A. Technical Note TN-97-32b. Swedish Nuclear Fuel and Waste Management Company.

Follin, S., Hermanson, J., Wei, L., Stigsson, M., 1998. Discrete fracture network parameters for the TRUE Block Scale Project. Summary of initial estimations and preliminary hydraulic observations. Technical Note TN-98-31b Swedish Nuclear Fuel and Waste Management Company.

Hermanson, J., Follin, S., Wei, L. 1997. Indata for discrete feature network modelling of the TRUE Block Scale site. Part 1- structural analysis of fracture traces in boreholes KA2563A and KA3510Anand in the TBM tunnel. Technical Note TN-97-31b Swedish Nuclear Fuel and Waste Management Company.

La Pointe, P., P. Wallman, W. Dershowitz, 1993. Stochastic estimation of fracture size through simulated sampling. Int. J. Rock Mech. Min Sci. & Geomech. Abstr. Vol 30, No. 7, pp. 1611-1617.

La Pointe, P., P. Wallmann, and S Follin (1995) Estimation of effective block conductivities based on discrete network analyses using data from the Äspö site, SKB TR 95-15, Swedish Nuclear Fuel and Waste Management Company, Stockholm.

Munier, R. (1995) Studies of geological structures at Äspö - Comprehensive summary of results, SKB PR 25-95-21, Swedish Nuclear Fuel and Waste Management Company, Stockholm.

Rhén, I., Gustafson, G., Stanfors, R., Wikberg, P., 1997. Äspö HRL- Geoscientific Evaluation 1997/5, models based on site characterisation 1986-1995. SKB TR 97-06. Swedish Nuclear Fuel and Waste Management Company.

Rhén, I., Forsmark, T, 1998. Prototype repository. Hydrology - Drill campaign 1. Äspö Hard Rock Laboratory Progress Report PR HRL-98-12. Swedish Nuclear Fuel and Waste Management Company.

Svensson, U., 1997. A site scale analysis of groundwater flow and salinity distribution in the Äspö area. SKB TR 97-17. Swedish Nuclear Fuel and Waste Management Company.

Terzaghi, R. D. (1965) Sources of error in joint surveys. Geotechnique, 15, pp. 287-304.

Yow, J. L., (1987) Blind zones in the aquisition of discontinuity orientation data. International Journal of Rock Mechanics and Mining Sciences and Geomechanics Abstracts, Technical Note, 24, No. 5, pp. 317-318.

Appendix A

Excerpt From The FracMan and MAFIC User Documentation

A.1 FracMan

FracMan is a software package developed by Golder Associates Inc. to model the geometry of discrete features, including faults, fractures, paleochannels, karsts and stratigraphic contacts. For convenience, all discrete features will be frequently referred to as fractures in this manual, although the tools provided in FracMan are equally useful for all types of discrete features.

FracMan is designed to provide geologists and engineers with an easy-to-use tool for modelling fractured rock masses, rock mechanics and hydrologic applications in hazardous and nuclear waste management, underground construction, mining and petroleum reservoir engineering. FracMan provides an integrated environment for the entire process of discrete feature data analysis and modelling. FracMan provides:

- **data analysis features** to allow transformation of raw data into the formats needed for discrete fracture modelling,
- **stochastic simulation** of fracture patterns to facilitate three-dimensional visualisation,
- **exploration simulation,** to improve the design and interpretation of site characterisation programs for collection of fracture data,
- **finite element mesh generation and output post-processing,** to facilitate flow and transport modelling in networks of fractures and
- **macro** support, to facilitate **Monte Carlo** stochastic simulation.

FracMan's data analysis capabilities include new techniques for analysing fracture orientation, size, intensity and transmissivity. These techniques provide the data needed for fracture geometric modelling from data which are frequently collected as part of comprehensive site investigations, but are rarely used in hydrologic or mechanical modelling.

FracMan's geometric modelling features include nine conceptual models for fracture heterogeneity. These models provide users with the flexibility to include fractal, non-stationary Poisson point process and correlated fracture locations. Geometric realism is enhanced by the ability to model terminations at fracture intersections, plus dislocation and rotation on faults.

A.1.1 FracSys: Fracture Data Analysis

FracMan discrete fracture modelling is useful for modelling possible geological conditions when there is little or no data. It is also useful for modelling *in situ* conditions when data is available. Unfortunately, FracMan requires information in formats which are frequently not available as part of conventional data collection programs, although these formats can be derived by appropriate procedures. The FracSys module provides those procedures.

A.1.1.1 ISIS: Interactive Set Identification System

ISIS defines fracture sets from field data using an adaptive, probabilistic pattern recognition algorithm. ISIS allows the user to select the fracture properties of concern and define their relative significance for the analysis. Unlike conventional approaches to fracture set definition, which define sets by contouring orientations on stereoplots, ISIS is as powerful for overlapping fracture sets as for clearly defined sets. The premise of the ISIS approach for definition of fracture sets is that the sets should be groups of fractures with similar properties. Orientation does not need to be the only property defining sets; size, termination, fillings and other properties can identify sets as well.

ISIS identifies fracture sets using multiple fracture properties. ISIS calculates the distribution of properties for the fractures assigned to each set, then re-assigns fractures to sets according to probabilistic weights proportional to their similarity to other fractures in the set. The properties of the sets are then recalculated and the process is repeated until the set assignment is optimised.

Assigning fractures to sets

The goal of the ISIS approach is to assign groups of fractures which are similar geologically or hydrogeologically to sets which are statistically homogenous . This is achieved by deriving the statistical properties of each set from the statistical properties of the fractures assigned to the set and then removing and reassigning fractures which have a low probability of being part of the set. The ISIS algorithm begins by requiring the user to select and assign weighting factors w_j to each of the n_j fracture characteristics of concern and to provide initial guesses for the properties of the each set k. In addition, the user must specify the convergence method, either hard sector, soft sector, sector preconditioning or none (see below). For each fracture i, ISIS then calculates a probability that the fracture belongs to that set. During the first iteration, this probability is calculated using the value of the probability density function for that property and set, taken at the value of the fracture.

$$P[i \in k] = C\, p_{w,k}$$

$$p_{w,k} = \sum_{j=1}^{n_j} W_j f_j(k_i) P_{si} + f_{si}$$

$$C = 1 \Big/ \sum_{k=1}^{n_k} p_w$$

where $P[i \in k]$ is the probability that fracture i is an element of set k, $p_{w,k}$ is the weighted probability density function of set k for property j, $f_k(k_i)$ is the probability density function of set k for property j evaluated for fracture i, w_j is the user-assigned weighting for property I and P_{si} and f_{si}; are sector factors, (see below) and C is a proportionality constant defined to ensure that the sum of probabilities for all set equals 1. ISIS does not require complete information on every fracture property j for all fractures i. When a piece of information about fracture i is missing, $f_k(k_i)$ is set at 0 for

that fracture over all sets k, such that only those properties for which values are specified are used in the assigning that fracture to a set.

The probability density functions $f_k(k_i)$ for each property of each set are provided by the user for the first iteration. For subsequent iterations, they are calculated using the distributional forms specified by the user, with moments calculated using the fractures assigned to sets during the previous iteration. The form of the probability density function $f_k(k_i)$ is also determined by the user and may be Fisher (for orientation), normal, lognormal, exponential or a histogram and is dependent on the property.

The factors P_{si} and f_{si} depend on the user-specified convergence method. Sectors are defined by the closest mean pole (or dip vector) as defined by the fracture set mean pole (or dip vector).

Table 3-2 Convergence Factors and Sectoring in ISIS

	Fracture i in same sector as set k mean pole (or dip)	Fracture i in different sector from set k mean pole (or dip)
Hard Sector	$P_{si} = 1$ $f_{si} = 0$	$P_{si} = 0$ $f_{si} = 0$
Soft Sector	$P_{si} = 1$ $f_{si} = 0.25$	$P_{si} = 1$ $f_{si} = 0$
No Sector	$P_{si} = 1$ $f_{si} = 0$	$P_{si} = 1$ $f_{si} = 0$
Sector Preconditioning	Same as Hard Sector first iteration Same as No Sector afterwards	

Once the probability $P[i \in k]$ has been calculated for each fracture and set, the fractures are reassigned to sets by Monte Carlo simulation, such that the each fracture is assigned to set k with probability $P[i \in k]$.

When all fractures have been reassigned to sets, the set distribution parameters are recalculated for each property j using the fractures assigned to that set. For orientation statistics, the mean pole vector or mean dip vector and the Fisher dispersion parameter k (Fisher et al., 1987) are calculated. For continuous distributions such as lognormal and normal, the mean and standard deviation are recalculated and for histogram distributions the percentages for each class are calculated. For example, for rock type histogram distributions, the property statistics for rock-type for set k are set to the percentage of each rock type among the fractures currently assigned to set k.

When the distributions of fracture properties for each set have been recalculated, ISIS repeats the process, reassigning sets to fractures. In order to speed convergence, a relaxation factor γ is used in calculating the probability $P[i \in k]$. This relaxation factor controls the rate of change in $P[i \in k]$ using a weighted average of probability density functions for the fractures current and previous set assignments:

$$P[i \in k] = Cp_{w,k}$$

$$p_{w,k} = \sum_{j=1}^{n_j}(1-\gamma_j)W_j f_j(k_i) + \sum_{j=1}^{n_j}\lambda_j W_j f_j^{(old)}(k_i)$$

$$C = \frac{1}{\sum_{k=1}^{n_k} p_w}$$

where $f_j^{(old)}$ is the probability density function from the previous iteration. For each property j, a relaxation factor of 0 calculates the probability $P[i \in k]$ based solely upon the current assignment of fractures to sets and a relaxation factor of 1 calculates the probability $P[i \in k]$ without an change as fractures are reassigned and as set-properties change. A value of approximately 0.5 is appropriate for most properties.

ISIS also uses damping factors in the calculation of updated mean directions and dispersion parameters for each set using the equation

$$\kappa^{(updated)} = (1-d_\kappa)\kappa^{(old)} + d_\kappa \kappa^{(new)}$$

$$\upsilon^{(updated)}(\bar{\varphi},\bar{\theta}) = \frac{(1-d\upsilon)\,\upsilon^{(old)}(\bar{\varphi},\bar{\theta}) + d\upsilon\,\upsilon^{(new)}(\bar{\varphi},\bar{\theta})}{\left|(1-d\upsilon)\,\upsilon^{(old)}(\bar{\varphi},\bar{\theta}) + d\upsilon\,\upsilon^{(new)}(\bar{\varphi},\bar{\theta})\right|}$$

where

d_κ	=	is the damping parameter for Fisher dispersion
d_υ	=	the damping parameter for mean orientation
$\kappa^{(old)}$	=	the Fisher dispersion parameter from the previous iteration.
$\kappa^{(new)}$	=	the Fisher dispersion parameter based on the fractures currently assigned set
$\kappa^{(updated)}$	=	the Fisher dispersion parameter to be used by the set in the next iteration.
υ	=	the unit vector for mean orientation (φ,θ).

This process is repeated for a number of iterations specified by the user. When the analysis is complete, ISIS calculates the Kolmogorov-Smirnov goodness-of-fit statistics for each of the properties and distributions used in the analysis, based upon the fractures assigned to the sets at the end of the analysis. This process of regrouping the fractures is repeated until the distribution parameters of the sets stabilise.

This algorithm has been verified utilising one, two and three overlapping Fisher distributed fracture sets.

Terzaghi Correction

ISIS includes the option to apply a modified Terzaghi correction (Terzaghi, 1965), to partially compensate for orientation bias of planar (trace plane) and linear (scan line and borehole) sampling. When the Terzaghi correction option is selected, the data set is modified so that for each original fracture data record, N records are added according to:

$$N = min(\lfloor R / cos\beta \rfloor, U)$$

where

R	=	a uniform, random deviate between 0 and 1,
β	=	the angle between the normal to the fracture plane and the borehole or scanline direction.
U	=	User-specified maximum correction.

This correction increases the number of records for fractures that have normal vectors at high angle to the direction of the borehole or scanline by a quantity that is inversely proportional to the probability of intersecting those fractures with the borehole or scanline.

A maximum value of N = 7 will avoid excessively strong correction for fractures that are nearly parallel to the boreholes or scanlines.

A.1.1.2 HeterFrac

HeterFrac geologic structure analysis allows the evaluation of single trace planes containing both linear and curved fracture traces.

HeterFrac derives statistics for seven of the geologic conceptual models implemented in FracMan/FracWorks for geologic simulation: Baecher Model, BART Model, geostatistical, POCS, Nearest Neighbour Model, Fractal ("Levy-Lee") Model and War-Zone Model. This section describes the models analysed and the statistical tests used for evaluation of the appropriateness of the different models.

HeterFrac Trace Analysis can be carried out using either trace centres or random points on the trace as measures for fracture location. HeterFrac prompts the user for specification of the trace using either trace centre or random point(s) before proceeding to analyse options. In general, no more than one random point should be used.

HeterFrac then provides six alternative selections:

- **Statistics** produces statistical analysis of trace maps, except for the calculations and goodness of fit tests for the Enhanced Baecher Model Poisson (uniform location) assumption and the box fractal dimension.

- **Baecher Analysis** calculates the box fractal dimension and uses the χ^2 test and the correlation coefficient to test the statistical significance of the Enhanced Baecher model's Poisson assumption and the box fractal dimension fit. When running the Baecher analysis, the user must specify the region to be analysed and the grid size to be used in calculating local fracture intensity P_{22}.

- **Geostatistical POCS** calculates the variogram for local fracture intensity P_{22} and determines the variogram fractal dimension D_v and the spherical variogram

correlation length λ, for the random field of local intensities. A non-linear least-squares algorithm is used to derive D_v and λ_v. The variogram fractal dimension D_v can be used with the POCS geometric conceptual model. The variogram correlation length λ, can be used with the POCS and geostatistical conceptual models.

- **Nearest Neighbour Analysis** calculates the relationship between fracture intensity P_{22} and the distance to user-defined major fractures using the χ^2 test and the correlation coefficient to determine the significance of the fit.

- **Levy-Lee Analysis** calculates the log-linear intensity P_{21} versus circle radius relationship for the box fractal dimension and uses the χ^2 test and correlation coefficient to determine the significance of the fit. The Levy-Lee analysis requires specification of the centre of the area to be analysed and the radiis of the smallest and largest circle to be used.

- **War Zone Analysis** calculates the relationship between the war zone criterion W_z and relative fracture intensity factor W_f. The region to be analysed and the grid cell size are specified as in the Baecher analysis. In addition, the user must specify values of war zone coefficients z_L, z_p and z_c. For deterministic war zone analysis, the user have to define the perimeter of a war zone. The program will then display the war zone intensity W_f and war zone criteria W_z for regions selected.

The determination of which spatial model that is most appropriate is accomplished in FracMan by means of statistical tests and geometrical measures such as the χ^2-test and the box fractal dimension. For example, a χ^2-test can be used to compare the observed distribution of fracture centres to a theoretical Poisson distribution. A significance of 85% or greater generally indicates a good fit to the Poisson distribution and a high probability that the Beacher model is appropriate. The box fractal dimension is a measure of how completely the fracture pattern fills the trace plane surface. A fractal dimension near 1 indicates a very strongly clustered, heterogeneous pattern, whereas a dimension close to 2 indicates a more homogeneous, space filling pattern. Large fractal dimensions indicate Poisson type models whereas smaller dimensions indicate clustered models such as the Nearest neighbour , War zone or Levy-Lee fractal models.

A.1.1.3 FracSize Tracelength Simulation Module

The FracSize data analysis module is used to determine the distribution of fracture radii that gives the best match to the observed tracelength data. FracSize uses simulated sampling to take into account censoring, truncation and sampling bias.

FracSize starts with an .ORS file containing measured fracture radii, a .SAB file containing the specification of the sampling process used to collect each of the fractures in the .ORS file and an assumed distribution of fracture radii provided by the user. FracSize then simulates the sampling process, compares the simulated sample to the actual data in the .ORS file and displays a graphical and statistical summary of the comparison.

Two optimisation algorithms are available to provide an automated search of the fracture radius distribution. For the simulated annealing and conjugate gradient optimisation algorithms, FracSize varies the assumed distribution of fracture radius to improve the match between simulated and measured trace results, as measured by either Kolmogorov-Smirnov (K-S) or Chi-Squared (χ^2)/statistics. For each iteration, ' FracSize carries out five realisations of a specific fracture radius distribution and calculates the mean K-S and χ^2 statistics as the measure of the goodness-of-fit provided by that fracture radius distribution.

A.1.1.4 Oxfilet

The OxFilet ("**O**snes E**x**traction from **F**ixed-**I**nterval-**L**ength **E**ffective **T**ransmissivities") module is used to determine the transmissivity distribution and frequency of conductive fractures from packer test data by using an approach adapted from Osnes et al. (1988).

The method assumes that the net transmissivity of a test zone is equal to the sum of the transmissivities of the conductive fractures that intersect that test zone:

$$T_i = \sum_{j=1}^{n_i} T_{ij}$$

where T_{ij} is the apparent transmissivity of the ith packer interval, n_i is the number of conductive fractures in the ith interval, and T_{ij} is the transmissivity of the jth conductive fracture within the ith interval. Within any given interval, the number of conductive fractures, n_i, is assumed to be a random number defined by a Poisson distribution (Benjamin and Cornell, 1970):

$$f_n(n) = \frac{\bar{n}^n e^{-\bar{n}}}{n!}$$

where $\bar{n}$ is the Poisson process rate, which is equal to the expected value of n. The conductive fracture frequency is given by $f_c = n/L_i$, where L_i = the length of the test zone.

The distribution of fracture transmissivities is assumed to be independent within each packer interval, with a given distributional form. The distribution of T_i is the sum of a random number of random events, and is therefore a compound Poisson process (Feller, 1971). In this approach, the mean number of fractures in a given interval is defined by the Poisson distribution rate parameter, n, and the distribution of fracture transmissivities T_{ij} is described by a lognormal distribution with a mean and standard deviation, m_{logT} and s_{logT}.

For any given set of parameters describing the distribution of fracture transmissivity $f(T_{ij})$ and conductive fracture frequency f_c, the distribution of packer interval transmissivities $f(T_i)$ are found by Monte Carlo simulation, with the best fit value found

by a simulated annealing search routine. Simulated intervals that contain no conductive fractures, or that have values of T_i less than $T_{threshold}$, the lowest threshold transmissivity that could be reliably measured in the field, are assigned a transmissivity equal to $T_{threshold}$.

The intensity and transmissivity distributions for the conductive fractures are then estimated by finding the best match between the observed distribution of packer interval transmissivities $f(T_i)$ and the distribution of test zone transmissivities found by simulation for given fracture frequency and single-fracture transmissivity distributions. This match is found both visually and by comparison of Kolmogorov-Smirnov (K-S) or Chi-Squared statistics (χ^2).

The values of n, $\mu_{\log T}$ and $\sigma_{\log T}$ that provided the best K-S or χ^2 minimise D are taken to be the best estimates of those parameters.

MAFIC flow and transport simulations require that the fracture transmissivity used be the effective transmissivity through a fracture between the fractures intersecting the fracture ("cross-fracture transmissivity", T_{fi}). OxFilet provides three alternative interpretations for the relationship between T_{fi} and T_{ij}, the transmissivity seen in the fixed interval packer test.

- The packer test influences one fracture at a time, such that the transmissivity seen for each fracture T_{ij} is equal to the cross fracture transmissivity, T_{fi}.

The packer test is strongly influenced by the local fracture aperture near the borehole. In this case the transmissivity seen by the packer test is a small scale ("at-borehole") transmissivity, and the cross-fracture transmissivity T_{ij} must be found using a correlation of the form,

$$T_{ij} = \left(\frac{1}{B_f}\right) T_{fi}$$

In OxFilet, the proportionality constant Bf is described as a normally distributed random variable with mean and standard deviation provided by the user.

- The packer test influences a network with a number of interconnected fractures. In this case, the transmissivity seen by the packer test, T_{ij}, is a network transmissivity related to the cross-fracture transmissivity of a number of fractures. Assuming series flow through the n fractures influenced by the packer test, the relationship between T_{ij} and T_{fi} could be given approximately by,

$$T_{ij} = \frac{\overline{m}}{\sum_{i=1}^{\overline{m}} \frac{1}{T_{fi}}} \quad (3\text{-}1)$$

For this option, an additional parameter $\underline{m}$, the mean number of fractures per network seen by packer tests must be specified. The distribution of $\underline{m}$ may be constant or Poisson.

A.1.2 FracWorks

The FracMan package idealises fractures as planar and polygonal. The planarity simplification is adopted for three reasons: firstly, because little field data is available on non-planar fractures; secondly, because planar fractures are computationally far more tractable than undulating fractures; and thirdly, because for problems of concern the effects of fracture undulation can be approximated in a more tractable manner, e.g., as an increased coefficient of friction for mechanical problems, or as an adjusted transmissivity for hydrological problems.

The assumption of polygonal fractures is both realistic and useful, as it allows the approximate representation of a wide variety of fracture shapes by a single mathematical form. Considerations from fracture mechanics suggest that in homogeneous rock the general shape of an isolated fracture should be elliptical, as is assumed in the Baecher model (Baecher et al, *1977).* However, since rock is generally heterogeneous, perfectly elliptical fractures are unlikely, and in a practical sense no error is introduced by representing the ideal, elliptical fracture by a many-sided polygon of equivalent area. Dershowitz (1984) has noted, moreover, that observed fractures are generally polygonal due to terminations of the fractures at intersections with other fractures. The Veneziano model (Veneziano, 1979) and the Dershowitz model (Dershowitz, 1984) both treat fractures as polygons.

The current version of FracMan contains nine conceptual models for fractures:

- the Enhanced Baecher model, an extension of the Baecher model which provides for termination of fractures at intersections with pre-existing fractures;

- the Levy-Lee Fractal model, a stochastic model which uses a Levy Flight fractal process to produce clusters of smaller fractures around widely scattered, larger fractures;

- the Nearest Neighbour model, a semi-stochastic, pattern-based model which simulates the tendency of fractures to be clustered around major joints and faults by preferentially producing new fractures in the vicinity of earlier fractures; and

- the War Zone model, a semi-stochastic, pattern-based model which imitates the geometry of shear zones by preferentially producing fractures in the regions between subparallel, neighbouring fractures.

- the Non-Planar zone model, a semi-stochastic model which generates fractures with location and orientation varying according to a user defined non-planar surface.

- the Fractal Box model which uses a self-similar fractured field to define fracture initiation points, which may be either centres or random surface points.

- the Fractal POCS (Projection Onto Convex Sets) model which generates a random field of fracture initiation points (centers or surface points) (a) consistent with a user

specified fatal dimension, (b) consistent with a user specified variogram, and (c) conditioned to intensities at specified locations.

- the Geostatistical model, which generates a random field of fracture initiation points (centre or surface points) according to a specified spherical, exponential, or null variogram.

- the Poisson Rectangle model, simple version of the Enhanced Baecher Model, in which fractures are represented by rectangles with prescribed length and width, rather than as polygonal disks with an "effective radius". Location and termination are treated the same way as in the Enhanced Baecher model.

- the BART model, a version of the Enhanced Baecher model in which the fracture termination process is modified to improve computational efficiency.

The first four of these models are described in Geier, Lee, and Dershowitz, 1989. These models all generate polygonal fractures that may or may not terminate at intersections with other fractures. The models differ from one another only with regard to the spatial distribution of the fractures, and the interrelationship of fracture size and fracture location.

A.2 MAFIC

MAFIC (Matrix/Fracture Interaction Code) was developed by Golder Associates to simulate transient flow and solute transport through three-dimensional rock masses with discrete fracture networks. Flow and solute transport are simulated in both the fractures and the rock matrix. MAFIC is part of the FracMan discrete feature analysis package. MAFIC provides flow and transport simulation for hydrogeological conceptual models generated under FracMan/FracWorks. Input files for MAFIC can be generated by FracMan/MeshMaker and FracMan/MeshMonster, and edited by FracMan/EdMesh.

MAFIC simulates flow in fractures using three-dimensional networks of triangular finite elements. MAFIC simulates flow in the rock matrix using either a fully discretized multi-dimensional Galerkin finite element approach, or a generic matrix block scheme. The matrix block scheme can use either one-dimensional finite elements or a pseudo steady-state analytical approximation. The matrix block approach reduces computational effort significantly, and is preferred for most applications, even though it does not model flow between non-intersecting fractures by matrix interconnection.

MAFIC simulates solute transport using a connective particle tracking approach. Solute dispersion is simulated stochastically using orthogonal, normally distributed, lateral and transverse dispersion vectors. MAFIC solute transport includes matrix diffusion, mineralspecific retardation, and sorption features.

MAFIC was designed to simplify input data requirements while providing maximum flexibility for the designation of boundary conditions. Input files may be specified by the user or generated by the FracMan fracture network simulation package. An efficient

iterative matrix solver is provided to maximise solution efficiency and minimise matrix storage requirements.

Initial development of MAFIC was funded by Battelle's Office of Waste Technology Development (OWTD). Development of the current version of MAFIC was funded primarily

Several researchers have shown that, in many cases, flow and solute transport through fracture networks cannot be accurately modelled with equivalent porous media models (Long, et. al., 1982; Robinson, 1984; Anderson and Deverstorp, 1987; Smith and Schwartz, 1984). To provide for more realistic simulations of fractured rock masses, flow models incorporating networks of discrete fractures are required. MAFIC is a finite element flow model designed to simulate transient flow and solute transport in a rock mass with a discrete fracture network.

MAFIC models fracture flow through a network of interconnecting "plates," and matrix flow through a three-dimensional volume. MAFIC is capable of handling very general fracture network geometries. Both constant and time-dependent Dirichlet (prescribed head) and Neumann (prescribed flux) flow boundary conditions can be specified at any network node. Time-varying solute source strengths may be prescribed as a specified concentration at a given fracture element node or boundary surface.

MAFIC provides a number of special features including:

1. Choice of linear or quadratic elements using the same input data. Linear elements are transformed into quadratic elements by automated insertion of midside nodes.
2. Simulation of matrix flow using either a fully discretized finite element procedure, or a generic matrix block scheme which can accommodate a variety of fracture geometries. The matrix block approach can reduce computation time by orders of magnitude.
3. Specification of nodal groups with identical time-varying head or flux boundary conditions. An option also exists for simulating wells (or other prescribed flux boundaries) containing several fracture and matrix nodes for which only the **total** timevarying well flux is known.
4. An efficient incomplete Choleskii conjugate gradient equation solver, which significantly reduces memory and computation time requirements.
5. Creation of a restart input file using nodal heads from the last timestep as initial heads to allow for changes in boundary condition type and location.
6. Capacity for multiple simulations with different fracture network geometries but identical problem parameters and boundary conditions to accommodate stochastically generated fracture networks.
7. Solute transport modelling with either steady-state or transient flow conditions and stochastic emulation of convective dispersion, matrix diffusion, radioactive decay, and mineral-specific retardation.

Appendix B

Transformations of the Log-Normal Distribution

The log-normal distribution is given by the function

$$f(x) = \frac{1}{x \ln(10) y_\alpha \sqrt{2\pi}} \exp\{-\frac{1}{2}(\frac{\log x - \bar{y}}{y_\alpha})^2\}$$

Where $\bar{y}$ and y_α is mean and standard deviation in $\log_{10}$ space. In FracMan the logarithmic distribution is defined by the mean and standard deviation in real space (arithmetic). This is to provide a mean in units of meters which is a comprehensible measure of fracture size. This is despite the fact that the standard deviation in real space is more complex to understand. There exists simple conversion formulas between $\log_{10}$ space and real space. Given the y and y_α the arithmetic mean $\bar{x}$, and standard deviation x_α is

$$\bar{x} = e^{(c\bar{y} + 1/2(cy_\alpha)^2}$$

and

$$x_\alpha = \bar{x}\sqrt{e^{(cy_\alpha)^2} - 1}$$

and vice versa, i.e. given $\bar{x}$ and x_α

$$\bar{y} = \frac{1}{c}(\ln(\bar{x}) - \frac{(cy_\alpha)^2}{2})$$

$$y_\alpha = \frac{1}{c}\sqrt{\ln(1 + (\frac{x_\alpha}{\bar{x}})^2)}$$

where c is the natural log of 10 (≈ 2.302).

APPENDIX C

Transmissivity histograms

KI0025F - Transmissivity from flow logging data (L=5m)

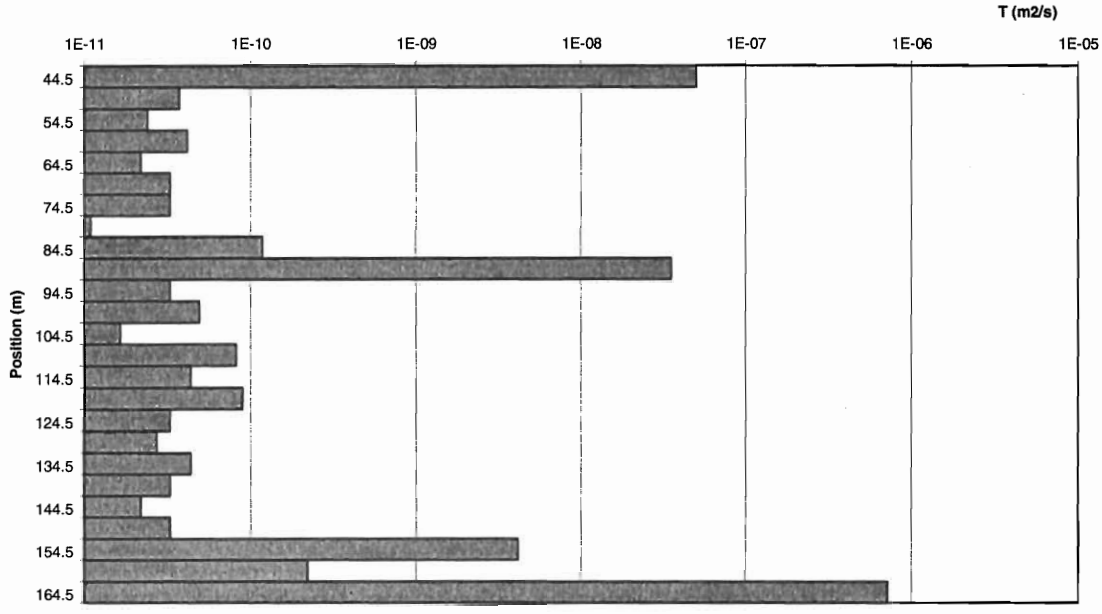

KA2511A - Transmissivity from flow logging data (L=5 m)

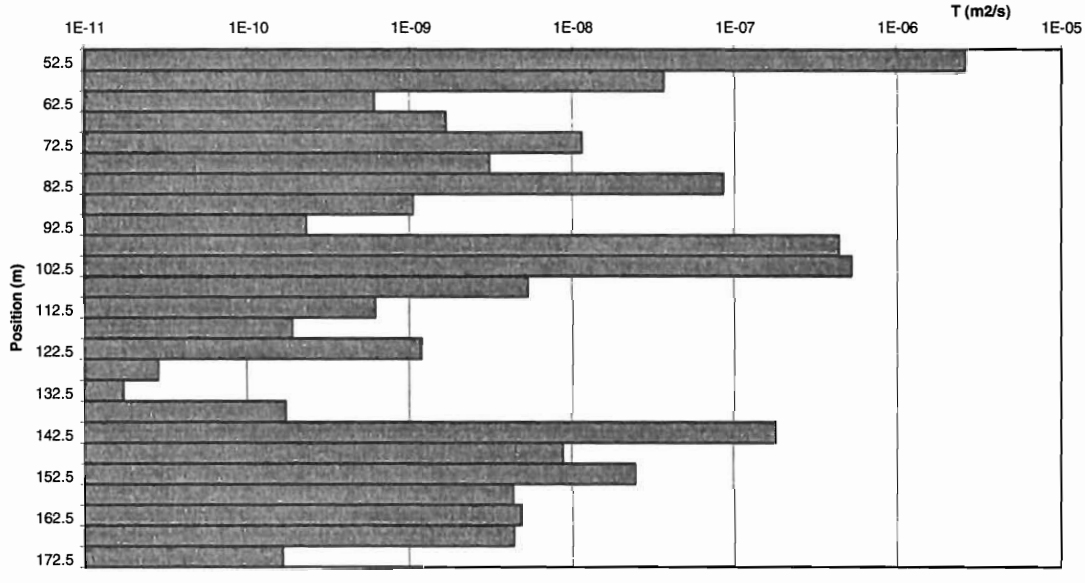

KA2563A - Transmissivity from flow logging data (L=5m)

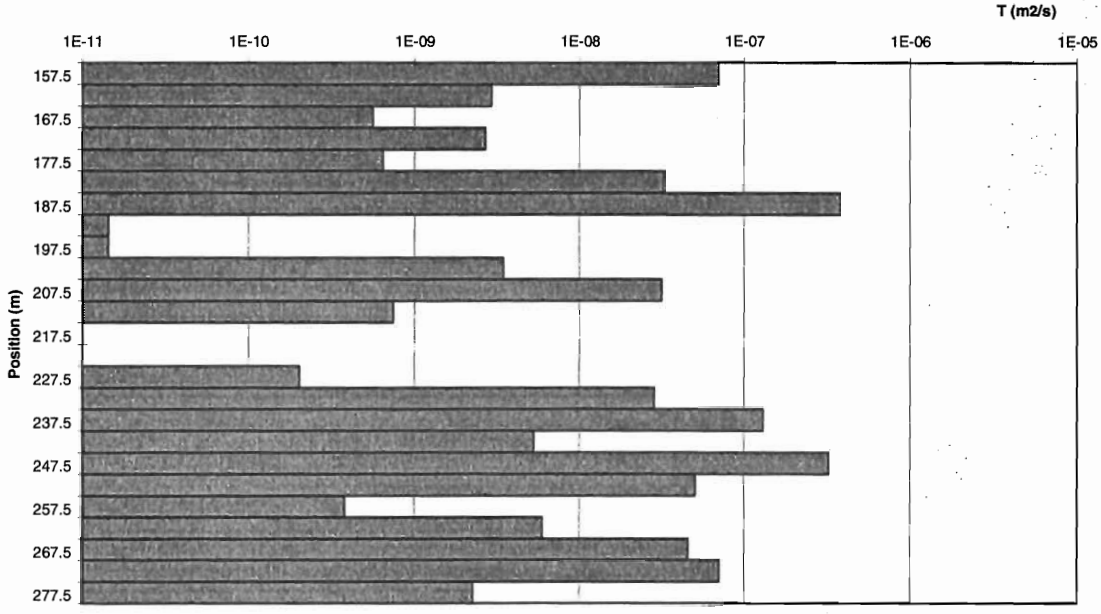

KA3510A - Transmissivity from flow logging data (L=5m)